UDK 536.75; PACS 47.70, 61.20.J

GENERALIZED COLLECTIVE MODES OF A LENNARD-JONES FLUID. HIGH MODE APPROXIMATION

I. P. OMELYAN, I. M. MRYGLOD

Institute for Condensed Matter Physics of the Ukrainian National Academy of Sciences, 1 Svientsitskii St., UA–290011 Lviv, Ukraine

Received March 20, 1995

The generalized collective mode approach proposed for the investigation of time correlation functions of a dense fluid is now extended to higher-order approximations. The generalized collective mode spectra of a Lennard-Jones fluid have been calculated for longitudinal fluctuations up to the nine-mode description and also for transverse fluctuations up to the four-mode description using molecular dynamics. The results are obtained as functions of wave vector. For longitudinal fluctuations four new kinetic modes are found in addition to five modes known previously. For transverse fluctuations we found the generalized hydrodynamic and three kinetic modes. A comparison of previous works with the results of lower-order approximations has been made.

1. Introduction

Recently, a conception of generalized collective modes for the investigation of time correlation functions (TCFs) of a dense fluid has been proposed by Cohen, de Schepper *et al* [1,2] and developed in computer-adapted form [3]. The generalized mode description can be considered as a generalization of the hydrodynamic models of a fluid [4-9] with the intent of constructing a generalized hydrodynamic theory which is exact in the hydrodynamic limit (the small values of wave-vector k and frequency ω) and a reasonable approximation for large k and ω. The proposed approach appears to be particularly promising in the context of developing methods of computer simulations as it enables one to obtain the self-consistent description of dynamical properties, using computer experiment data for lower-order TCFs or, as an alternative, for static correlation functions (SCFs).

In the generalized mode approach the TCFs are represented as the sum of partial terms, each being associated with the corresponding collective excitation may be simply written via the eigenvector and eigenvalue of a generalized operator of evolution. Certain of the generalized collective modes can be considered as extensions of the usual hydrodynamic modes [7,8] and tend to the well-known results in the hydrodynamic limit. In particular, it was shown [2] that for longitudinal fluctuations three generalized collective modes corresponding to the lowest eigenvalues reduce to the heat and two sound modes, the eigenvalues of which vanish when k

goes to zero. The other (nonhydrodynamic) ones are kinetic modes and lead to the finite damping coefficients in the hydrodynamic limit. In addition to three generalized hydrodynamic modes, two kinetic ones have been found [2] with the use of five-mode description by molecular dynamics (MD) simulations. These results were obtained for a Lennard-Jones (LJ) liquid as the solution of the equations for TCFs in a Markovian approximation. The higher-order SCFs were calculated by numerical differentiation of the MD time correlation functions. The density-density, energy-energy, density-energy and longitudinal momentum-momentum TCFs have been obtained by MD simulations. From a weighted least-squares-fitting procedure the memory functions (or the transport coefficients) that gave the best fit to the MD correlation functions have been evaluated. The 5×5 TCFs were found [2] in terms of the SCFs and the matrix of the generalized evolution each element of which depends upon k but not upon t.

Thereafter, the natural question about influence of the next approximations on the generalized mode spectrum and the results for TCFs arises. As follows from mathematical treatment, the full spectrum of the generalized evolution operator have to describe the TCFs exactly. This makes the investigation of the generalized modes in higher approximations all the more important. In [3] we developed the previous approach [2] and as a result the generalized collective mode spectra have been calculated for longitudinal fluctuations in the seven-mode description and for transverse fluctuations up to the three-mode description. It was shown that seven- (instead of five-) mode approximation led to calculation of dynamical structure factor with more accuracy. It must be emphasized that our method [3] of calculations differs from [2] in two main points. First, the all SCFs functions were calculated at once by MD simulations with the aim to avoid the additional errors from the numerical differentiation. Second, the memory functions in Markovian approximation could be presented via the hydrodynamic correlation times and the SCFs for arbitrary set of dynamic variables. The hydrodynamic correlation times were also found by MD simulations. This means our scheme is free of any adjustable parameters and for studying of the next approximation it is necessary only to find the corresponding higher-order SCFs.

Moreover, it is interesting to apply the generalized mode approach for the investigation of the transverse fluctuations and to consider the question of the propagating excitation existence discussed previously in the literature [7,8,15]. It is the goal of this paper to solve some problems stated above.

In this article, developing the method proposed in [3], we made a next step in the investigation of high-mode approximations and considered nine- and four- mode descriptions for longitudinal and transverse fluctuations, respectively. It was shown that such high-mode approximations provide an excellent agreement with MD data for TCFs and generalized transport coefficients. The generalized collective modes are evaluated using our MD data for the SCFs and hydrodynamic correlation times.

The outline of this paper is as follows. In Sec. 2 the set of dynamic variables, the general properties of the TCFs, and MD experiment are described. The equations for the longitudinal and transverse TCFs as well as the results for the collective mode spectra are presented in Sec. 3. Results of calculation for the TCFs, dynamic structure factor and the generalized transport coefficients are given in Sec. 4.

2. Time correlation functions

2.1. General properties

Let us consider a spatially homogeneous, isotropic system of N identical point classical particles of mass m in volume V. We introduce operators of densities of particles' number n, momentum $\boldsymbol{J}$ and energy e:

$$\hat{n}(\boldsymbol{r},t) = \sum_{i=1}^{N} \delta(\boldsymbol{r} - \boldsymbol{r}_i(t)) \,, \tag{2.1}$$

$$\hat{\boldsymbol{J}}(\boldsymbol{r},t) = \sum_{i=1}^{N} m\boldsymbol{v}_i(t)\delta(\boldsymbol{r} - \boldsymbol{r}_i(t)) \,, \tag{2.2}$$

$$\hat{e}(\boldsymbol{r},t) = \sum_{i=1}^{N} e_i(t)\delta(\boldsymbol{r} - \boldsymbol{r}_i(t)) \,, \tag{2.3}$$

where

$$e_i(t) = \frac{m\boldsymbol{v}_i^2(t)}{2} + \frac{1}{2}\sum_{j=1(j\neq i)}^{N} \Phi_{ij}(t) \,, \tag{2.4}$$

$\boldsymbol{r}_i(t)$ and $\boldsymbol{v}_i(t)$ denote the position and velocity, respectively, of particle i at time t. $\Phi_{ij}(t) \equiv \Phi(r_{ij}(t))$ is a potential of interparticle interaction and $r_{ij}(t) = |\boldsymbol{r}_i(t) - \boldsymbol{r}_j(t)|$. For a closed system in the microcanonical ensemble the total number of particles, the total momentum and the total energy remain constants, i.e.

$$\int_V \hat{n}(\boldsymbol{r},t)d\boldsymbol{r} = N \,, \tag{2.5}$$

$$\int_V \hat{\boldsymbol{J}}(\boldsymbol{r},t)d\boldsymbol{r} = \boldsymbol{J} \,, \tag{2.6}$$

$$\int_V \hat{e}(\boldsymbol{r},t)d\boldsymbol{r} = E \,. \tag{2.7}$$

By performing the spatial Fourier transformation, one can obtain the following set of hydrodynamic microscopic variables in $\boldsymbol{k}$-representation

$$A(\boldsymbol{k},t) \equiv \{n(\boldsymbol{k},t), \boldsymbol{J}(\boldsymbol{k},t), e(\boldsymbol{k},t)\} = \{A_i(\boldsymbol{k},t)\} \,, \tag{2.8}$$

where

$$n(\boldsymbol{k},t) = \frac{1}{\sqrt{N}}\int_V \hat{n}(\boldsymbol{r},t)\exp(i\boldsymbol{k}\boldsymbol{r})d\boldsymbol{r} = \frac{1}{\sqrt{N}}\sum_{i=1}^{N}\exp(i\boldsymbol{k}\boldsymbol{r}_i(t)) \,, \tag{2.9}$$

$$\boldsymbol{J}(\boldsymbol{k},t) = \frac{1}{\sqrt{N}}\int_V \hat{\boldsymbol{J}}(\boldsymbol{r},t)\exp(i\boldsymbol{k}\boldsymbol{r})d\boldsymbol{r} = \frac{1}{\sqrt{N}}\sum_{i=1}^{N} m\boldsymbol{v}_i(t)\exp(i\boldsymbol{k}\boldsymbol{r}_i(t)) \,, \tag{2.10}$$

$$e(\boldsymbol{k},t) = \frac{1}{\sqrt{N}}\int_V \hat{e}\,(\boldsymbol{r},t)\exp(i\boldsymbol{k}\boldsymbol{r})d\boldsymbol{r} = \frac{1}{\sqrt{N}}\sum_{i=1}^{N} e_i(t)\exp(i\boldsymbol{k}\boldsymbol{r}_i(t)) \,. \tag{2.11}$$

We also define the higher order kinetic microscopic variables $A^{(p)}(\boldsymbol{k},t)$ as p-fold time derivatives of the corresponding hydrodynamic variables

$$A^{(p)}(\boldsymbol{k},t) = \frac{d^p}{dt^p}A(\boldsymbol{k},t) \tag{2.12}$$

and consider the equilibrium time correlation functions

$$f_{ij}^{p,s}(\boldsymbol{k},t) \equiv \langle A_i^{(p)}(\boldsymbol{k},t)A_j^{(s)}(-\boldsymbol{k},0)\rangle = \langle A_i^{(p)}(\boldsymbol{k},0)A_j^{(s)}(-\boldsymbol{k},-t)\rangle \ , \tag{2.13}$$

where $i,j = n,\boldsymbol{J},e$ and $\langle\ \rangle$ denotes an equilibrium average.

Restricting an order of derivatives in (2.13) by the condition $p+s \leq q_{max}$, where $p,s = 0,1,2...$, and taking into account that $\boldsymbol{J}(\boldsymbol{k},t)$ is a vector with three scalar components, we can find that the $[5(q_{max}+1)]^2$ scalar combinations of functions $f_{ij}^{p,s}(\boldsymbol{k},t)$ are in all. Most of these functions may be expressed via other ones from this set. Therefore, it is convenient to separate a base set of functions in such a way that all others can be obtained from this set using a minimum of numerical operations. In order to do this we have to describe some properties of TCFs under consideration. The first group of properties is immediately evident from the definitions of dynamic variables (2.8)-(2.12) and the TCFs (2.13). It is easy to show that

$$f_{ij}^{p,s}(\boldsymbol{k},t) = f_{ji}^{s,p}(-\boldsymbol{k},-t) \ , \tag{2.14}$$

$$\mathrm{Re}f_{ij}^{p,s}(\boldsymbol{k},t) + i\mathrm{Im}f_{ij}^{p,s}(\boldsymbol{k},t) = \mathrm{Re}f_{ij}^{p,s}(-\boldsymbol{k},t) - i\mathrm{Im}f_{ij}^{p,s}(-\boldsymbol{k},t) \ , \tag{2.15}$$

$$f_{nl}^{p,s}(\boldsymbol{k},t) = \frac{i\boldsymbol{k}}{m}f_{\boldsymbol{J}l}^{p-1,s}(\boldsymbol{k},t) \ . \tag{2.16}$$

Furthermore, from (2.13) and properties of differential operations we obtain

$$f_{ij}^{p+p',s}(\boldsymbol{k},t) = \frac{\partial^{p'}}{\partial t^{p'}}f_{ij}^{p,s}(\boldsymbol{k},t) \ , \tag{2.17}$$

$$f_{ij}^{p,s}(\boldsymbol{k},t)|_{p+s=q} = (-1)^{|p-p'|}f_{ij}^{p',s'}(\boldsymbol{k},t)|_{p'+s'=q} \ . \tag{2.18}$$

The second group of properties follows from the fact that equations of motion and the equilibrium average are invariant with respect to time and coordinate inversions. Under time inversion the dynamic variables $A_i^{(p)}(\boldsymbol{k},t)$ transform to $\mu_i(-1)^p A_i^{(p)}(\boldsymbol{k},-t)$, where $\mu_i = \pm 1$, namely, $\mu_n = \mu_e = 1$ and $\mu_J = -1$. Hence we have that

$$f_{ij}^{p,s}(\boldsymbol{k},t) = \mu_i\mu_j(-1)^{p+s}f_{ij}^{p,s}(\boldsymbol{k},-t) \ . \tag{2.19}$$

Using coordinate inversion one can find that the dynamic variables $A_i^{(p)}(\boldsymbol{k},t)$ change to $\mu_i A_i^{(p)}(-\boldsymbol{k},t)$. Then we obtain

$$f_{ij}^{p,s}(\boldsymbol{k},t) = \mu_i\mu_j f_{ij}^{p,s}(-\boldsymbol{k},t) \ . \tag{2.20}$$

As evident from the properties (2.15) and (2.20), the functions $f_{ij}^{p,s}(\boldsymbol{k},t)$ are purely real for $\mu_i\mu_j = +1$ or purely imaginary for $\mu_i\mu_j = -1$. From the

properties (2.19) it is apparent that the TCFs are even or odd with respect to time depending on whether the sign of the factor $\mu_i\mu_j(-1)^{p+s}$ is plus or minus. Obviously, in the last case the corresponding SCFs are equal to zero. The property (2.18) gives the possibility to consider arbitrary one TCF only from the set of TCFs $f_{ij}^{p,s}(\boldsymbol{k},t)$ for which $p+s=q$. Combining the properties (2.14), (2.19), (2.20) and taking into account that $\mu_i^2=1$ always we find $f_{ij}^{p,s}(\boldsymbol{k},t)=(-1)^{p+s}f_{ji}^{s,p}(\boldsymbol{k},t)$, i.e. TCFs is symmetric or antisymmetric functions with respect to permutations of indexes.

Yet another group of properties for $f_{ij}^{p,s}(\boldsymbol{k},t)$ is connected with a separation of the longitudinal and transverse components of dynamic variables in an isotropic system. Let us direct for definiteness vector $\boldsymbol{k}$ along the Z-axis in the Cartesian system of coordinates. Since equations of motion are invariant with respect to particular coordinate inversion along one or two axis, it can easily be shown that among the TCFs constructed on the binary combinations of the components of vector quantities, nonzero elements will have only diagonal components. In our case we have $\langle A^x(\boldsymbol{k},t)A^x(-\boldsymbol{k},0)\rangle = \langle A^y(\boldsymbol{k},t)A^y(-\boldsymbol{k},0)\rangle$. If the TCF is constructed as the binary combination of a vector quantity and a scalar one, the nonzero result appears only for the Z-component. Finally, owing isotropy of the system time correlation functions do not depend on orientation of $\boldsymbol{k}$-vector and depend only on magnitude $k=|\boldsymbol{k}|$, i.e. $f_{ij}^{p,s}(\boldsymbol{k},t)\equiv f_{ij}^{p,s}(k,t)$.

Using all properties mentioned above, we can separate a minimum number of the TCFs, so that the rest of TCFs for which $p+s\le q_{max}$ are expressed according to (2.14)-(2.20) in terms of this base set by some simple manipulations. The choice of the base set TCFs is determined by the kinds of acceptable numerical manipulations. If we allow the differentiation in any order, the set of four TCFs can be used as the base set. For instance, using the set of TCFs f_{nn}, f_{ne}, f_{ee} and $f_{JJ}^{(T)}\equiv f_{J^xJ^x}=f_{J^yJ^y}$, the rest of ones can be expressed in terms of these functions as at most $(q_{max}+2)$-fold time derivatives. However, an additional complication is the functions are unknown in an explicit analytic form. Hereafter, we should determine these functions numerically by the MD method. Since in simulations the TCFs are commonly calculated with an accuracy, as a rule, no better than 1%, the numerical differentiation of approximately calculated functions leads to an appreciable increase of the error. For example, the computations showed the error may be as an order of magnitude or even worse, the four-fold time derivatives having been used. From this reason, if we want to have a reliable data for all functions, an extended base set of the directly calculating TCFs such that the rest of ones can be expressed in terms of this extended base set not using any differentiations for TCFs which are non-zero in the static limit or using only one-fold time derivatives for TCFs which are equal to zero in static limit is more preferable. Such extended base set in the case of $q_{max}=4$ may be chosen as follows

$$f_{nn}(k,t),\ f_{ne}(k,t),\ f_{ee}(k,t),\ f_{JJ}^{(L,T)}(k,t),\ f_{Je}^{(L)}(k,t)=if_{Je}^{(L)}(k,t),$$
$$f_{JJ}^{(L,T)}(k,t),\ f_{\dot{e}\dot{e}}(k,t),\ f_{J\dot{e}}^{(L)}(k,t)=if_{J\dot{e}}^{(L)}(k,t),\ f_{J\ddot{J}}^{(L,T)}(k,t),\ f_{\ddot{e}\ddot{e}}(k,t)$$

and includes the 13 TCFs, each of them is even with respect to time (nonzero in static limit). Among these functions, the 11 TCFs are pure real and

the 2 ones are pure imaginary. In such a way all $[5(q_{max}+1)]^2$ functions can been determined (see Table 1). The TCFs which are equal to zero in the static limit are displayed in Table 1 as proportional to one-fold time derivatives of corresponding functions from the base set.

Table 1. The time correlation functions $f_{ij}^{p,s}(k,t)$ for $p+s \leq 4$.

Non–zero part	ij/q	0	1	2	3	4
Re	nn	$f_{nn}(k,t)$	$\sim \dot{f}_{nn}(k,t)$	$\sim f_{JJ}^{(L)}(k,t)$	$\sim \dot{f}_{JJ}^{(L)}(k,t)$	$\sim f_{\dot{J}\dot{J}}^{(L)}(k,t)$
Im	nJ	$\sim \dot{f}_{nn}(k,t)$	$\sim f_{\dot{J}J}^{(L)}(k,t)$	$\sim \dot{f}_{\dot{J}J}^{(L)}(k,t)$	$\sim f_{\dot{J}\dot{J}}^{(L)}(k,t)$	$\sim \dot{f}_{\dot{J}\dot{J}}^{(L)}(k,t)$
Re	ne	$f_{ne}(k,t)$	$\sim \dot{f}_{ne}(k,t)$	$\sim f_{Je}^{(L)}(k,t)$	$\sim \dot{f}_{Je}^{(L)}(k,t)$	$\sim f_{J\dot{e}}^{(L)}(k,t)$
Re	JJ	$f_{JJ}^{(L,T)}(k,t)$	$\sim \dot{f}_{JJ}^{(L,T)}(k,t)$	$f_{\dot{J}\dot{J}}^{(L,T)}(k,t)$	$\sim \dot{f}_{\dot{J}\dot{J}}^{(L,T)}(k,t)$	$f_{\dot{J}\dot{J}}^{(L,T)}(k,t)$
Im	Je	$\sim \dot{f}_{ne}(k,t)$	$f_{Je}^{(L)}(k,t)$	$\sim \dot{f}_{Je}^{(L)}(k,t)$	$f_{\dot{J}e}^{(L)}(k,t)$	$\sim \dot{f}_{\dot{J}\dot{e}}^{(L)}(k,t)$
Re	ee	$f_{ee}(k,t)$	$\sim \dot{f}_{ee}(k,t)$	$f_{\dot{e}\dot{e}}(k,t)$	$\sim \dot{f}_{\dot{e}\dot{e}}(k,t)$	$f_{\dot{e}\ddot{e}}(k,t)$

The explicit expressions for the derivatives of dynamic variables (2.1)-(2.3) are

$$\dot{\boldsymbol{J}}(\boldsymbol{k},t) = \frac{d}{dt}\boldsymbol{J}(\boldsymbol{k},t) = \frac{1}{\sqrt{N}}\sum_{i=1}^{N}\{\boldsymbol{a}_i(t)+i(\boldsymbol{k}\boldsymbol{v}_i(t))\boldsymbol{v}_i(t)\}m\exp(i\boldsymbol{k}\boldsymbol{r}_i(t)), \quad (2.21)$$

$$\dot{e}(\boldsymbol{k},t) = \frac{d}{dt}e(\boldsymbol{k},t) = \frac{1}{\sqrt{N}}\sum_{i=1}^{N}\{\dot{e}_i(t)+i(\boldsymbol{k}\boldsymbol{v}_i(t))e_i(t)\}\exp(i\boldsymbol{k}\boldsymbol{r}_i(t)), \quad (2.22)$$

$$\ddot{\boldsymbol{J}}(\boldsymbol{k},t) = \frac{d^2}{dt^2}\boldsymbol{J}(\boldsymbol{k},t) = \frac{1}{\sqrt{N}}\sum_{i=1}^{N}\{\dot{\boldsymbol{a}}_i(t)-(\boldsymbol{k}\boldsymbol{v}_i(t))^2\boldsymbol{v}_i(t)+$$
$$+\ i[2(\boldsymbol{k}\boldsymbol{v}_i(t))\boldsymbol{a}_i(t)+(\boldsymbol{k}\boldsymbol{a}_i(t))\boldsymbol{v}_i(t)]\}m\exp(i\boldsymbol{k}\boldsymbol{r}_i(t)), \quad (2.23)$$

$$\ddot{e}(\boldsymbol{k},t) = \frac{d^2}{dt^2}e(\boldsymbol{k},t) = \frac{1}{\sqrt{N}}\sum_{i=1}^{N}\{\ddot{e}_i(t)-(\boldsymbol{k}\boldsymbol{v}_i(t))^2e_i(t)+$$
$$+\ i[2(\boldsymbol{k}\boldsymbol{v}_i(t))\dot{e}_i(t)+(\boldsymbol{k}\boldsymbol{a}_i(t))e_i(t)]\}\exp(i\boldsymbol{k}\boldsymbol{r}_i(t)), \quad (2.24)$$

where

$$\boldsymbol{a}_i(t) = \frac{d}{dt}\boldsymbol{v}_i(t) = \sum_{j=1(j\neq i)}^{N} \boldsymbol{a}_{ij}, \quad \boldsymbol{a}_{ij} = -\frac{1}{m}\Phi'(r_{ij})\frac{\boldsymbol{r}_{ij}}{r_{ij}} , \tag{2.25}$$

$$\dot{e}_i(t) = \frac{1}{2}\sum_{j=1(j\neq i)}^{N} m[\boldsymbol{v}_i(t) + \boldsymbol{v}_j(t)]\boldsymbol{a}_{ij} , \tag{2.26}$$

$$\dot{\boldsymbol{a}}_i(t) = \sum_{j=1(j\neq i)}^{N} \frac{1}{m}\left\{-\Phi'(r_{ij})\frac{\boldsymbol{v}_{ij}}{r_{ij}} - [r_{ij}\Phi''(r_{ij}) - \Phi'(r_{ij})]\frac{\boldsymbol{r}_{ij}(\boldsymbol{r}_{ij}\boldsymbol{v}_{ij})}{r_{ij}^3}\right\} , \tag{2.27}$$

$$\ddot{e}_i(t) = \frac{1}{2}\sum_{j=1(j\neq i)}^{N} \left\{m(\boldsymbol{a}_i + \boldsymbol{a}_j)\boldsymbol{a}_{ij} - \frac{(v_i^2 - v_j^2)}{r_{ij}}\Phi'(r_{ij}) - [r_{ij}\Phi''(r_{ij}) - \right.$$

$$\left. -\Phi'(r_{ij})]\frac{(\boldsymbol{v}_i + \boldsymbol{v}_j)\boldsymbol{r}_{ij}(\boldsymbol{r}_{ij}\boldsymbol{v}_{ij})}{r_{ij}^3}\right\} \tag{2.28}$$

and

$$\Phi'(r) = \frac{d\Phi(r)}{dr} , \quad \Phi''(r) = \frac{d^2\Phi(r)}{dr^2} , \quad \boldsymbol{v}_{ij} = \boldsymbol{v}_i - \boldsymbol{v}_j .$$

The microscopical expressions (2.21)-(2.24) and (2.25)-(2.28) were used for the MD simulations.

2.2. Molecular dynamics simulations

We have studied a system composed of $N = 256$ particles interacting through a cut-off Lennard-Jones potential $\Phi(r) \equiv \Phi_{LJ}(r, r_c)$ at constant volume $V = L^3$, where

$$\Phi_{LJ}(r, r_c) = \begin{cases} \Phi_{LJ}(r) - \Phi_{LJ}(r_c) & \text{if } r \leq r_c \\ 0 & \text{if } r > r_c \end{cases} \tag{2.29a}$$

and

$$\Phi_{LJ}(r) = 4\epsilon_{LJ}[(\sigma_{LJ}/r)^{12} - (\sigma_{LJ}/r)^6] \tag{2.29b}$$

is the exact LJ potential. The simulations have been performed at nearly the same thermodynamic point as considered in [2,3] for a reduced density $n^* = \frac{N}{V}\sigma_{LJ}^3 = 0.845$ and a reduced temperature $T^* = k_B T/\epsilon_{LJ} = 1.706$ with the aim to compare our results with the previous ones. We used $r_c = L/2$, where $L = \sigma_{LJ}(N/n^*)^{1/3} = 6.716\sigma_{LJ}$ is the length of the simulation box edge, so that $\Phi_{LJ}(r, r_c)$ was very close to the exact LJ potential.

In our MD experiment the toroidal boundary conditions were applied and the equations of motion were integrated using the Verlet algorithm.

in velocity form with a time increment of $\Delta t = 0.005\tau_\sigma$, where $\tau_\sigma = \sigma_{LJ}(m/\epsilon_{LJ})^{1/2}$. In order to ensure a stability of the full energy E of the system, where $E/(N\epsilon_{LJ}) = \frac{3}{2}T^* + u^*$ and $u^* = \langle U\rangle/(N\epsilon_{LJ}) = -4.765$ is a reduced potential energy per particle, velocities of particles were moderately adjusted by rescaling of the kinetic energy after every 100 time steps, so that deviations of E from the constant level did not exceed 0.14%. The simulations were started from fixed configuration of positions in the form of a face-centered cubic lattice and random velocities with the Maxwell distribution. The system was allowed to achieve equilibrium for $2 \times 10^4 \Delta t = 100\tau_\sigma$ time steps. The observation time over equilibrium state of the system was $2 \times 10^5 \Delta t = 1000\tau_\sigma$. Every 8-th configuration was taken into account in computation of equilibrium averages. The 13 basic TCFs were calculated directly by definition (2.13) with time step $2\Delta t = 0.01\tau_\sigma$ in the interval $\tau \in [0, 2\tau_\sigma]$ for $k = [1, 2, ..., 25]k_{min}$, where $k_{min} = 2\pi/L = 0.936/\sigma_{LJ}$.

The reduced static correlation functions

$$\bar{f}_{ij}^{p,s}(k) = f_{ij}^{p,s}(k)\ \tau_\sigma^{p+s}/x_i x_j$$

from the base set $p + s \leq 4$, where $x_n = 1$, $x_J = (m\epsilon_{LJ})^{1/2}$, $x_e = \epsilon_{LJ}$ and $f_{ij}^{p,s}(k) \equiv f_{ij}^{p,s}(k, t = 0)$, are presented as depending on wave-vector in Fig. 1 and Fig. 2 (a)-(c). These functions were calculated directly in MD simulations from definition (2.13). Static correlation function momentum-momentum is evaluated analytically

$$f_{JJ}^{(L,T)}(k) = mk_BT\ .$$

Additional static correlation functions

$$f_{\dddot{J}\ddot{e}}^{(L)}(k) = i\tilde{f}_{\dddot{J}\ddot{e}}^{(L)}(k)\ , \quad f_{\ddot{e}\ddot{e}}(k)\ , \quad f_{\dddot{J}\dddot{J}}^{(L,T)}(k)$$

for which $p+s = 6$ (Fig. 2 (d)-(f)), were calculated as two-fold time derivatives at $t = 0$ of the corresponding lower-order basic TCFs using the property (2.17):

$$f_{\dddot{J}\ddot{e}}^{(L)}(k) = -\lim_{t\to 0}\frac{\partial^2}{\partial t^2} f_{J\dot{e}}^{(L)}(k,t)\ ,$$

$$f_{\ddot{e}\ddot{e}}(k) = -\lim_{t\to 0}\frac{\partial^2}{\partial t^2} f_{\dot{e}\dot{e}}(k,t)\ ,$$

$$f_{\dddot{J}\dddot{J}}^{(L,T)}(k) = -\lim_{t\to 0}\frac{\partial^2}{\partial t^2} f_{\dot{J}\dot{J}}^{(L,T)}(k,t)\ .$$

As was mentioned above wave-vector-dependent quantities were calculated for the discrete set of $\boldsymbol{k}$-vectors accessible in the simulating. The values for investigated quantities in these grid points are shown in Figs. 1, 2 by circles. Solid lines represent an interpolation data for intermediate values between the grid points and extrapolation to $k = 0$. We reduced all SCFs presented in Figs. 1, 2 (except Fig. 1 (d)) in such a way that they are even functions with respect to wave-vector and accept finite non-zero values when $k \to 0$.

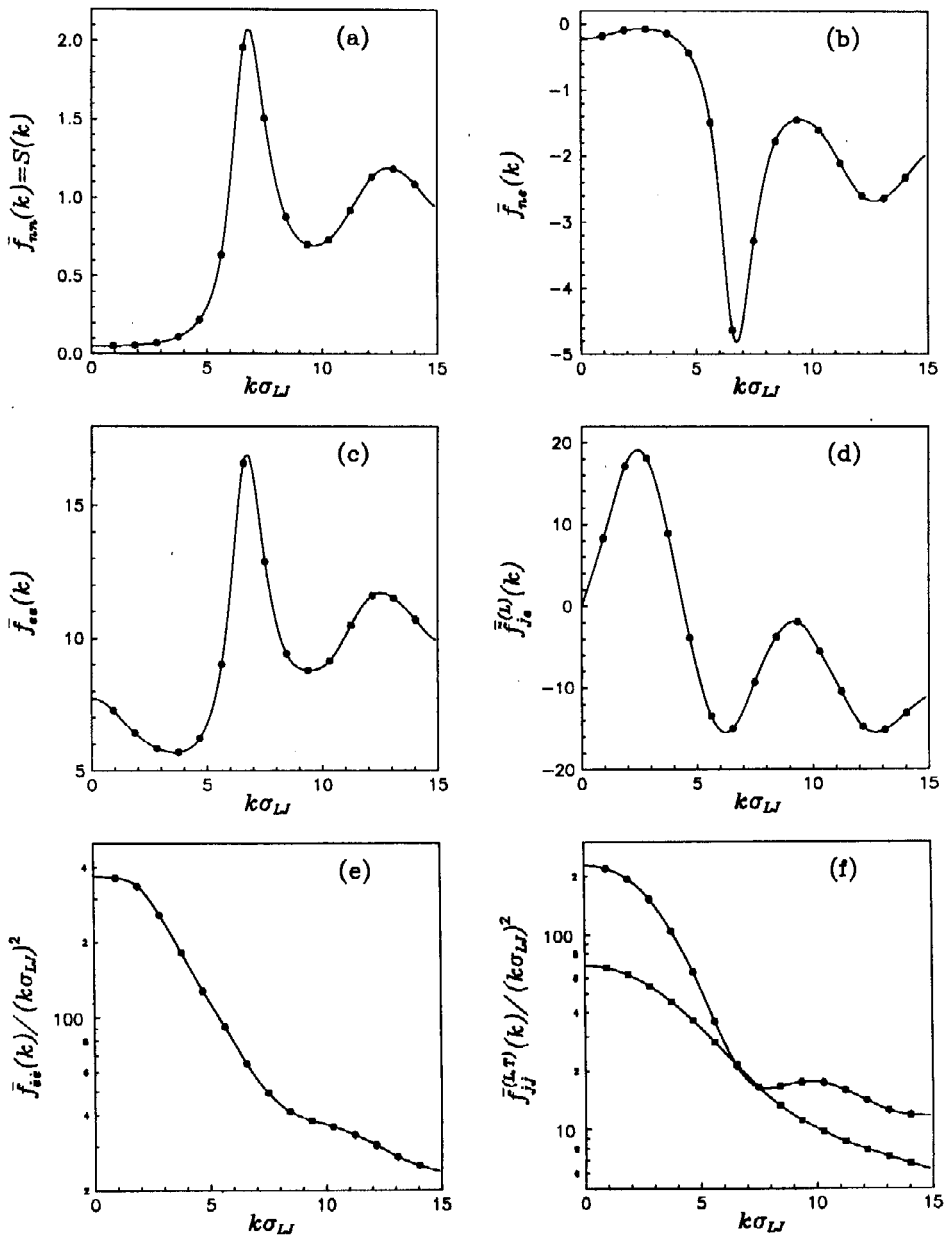

Fig. 1. MD results for the reduced static correlation functions versus wave-vector: **(a)** density-density; **(b)** density-energy; **(c)** energy-energy; **(d)** momentum-energy ($p = 1, s = 0$); **(e)** energy-energy ($p = s = 1$); **(f)** momentum-momentum ($p = s = 1$) longitudinal (upper curve) and transverse (lower curve).

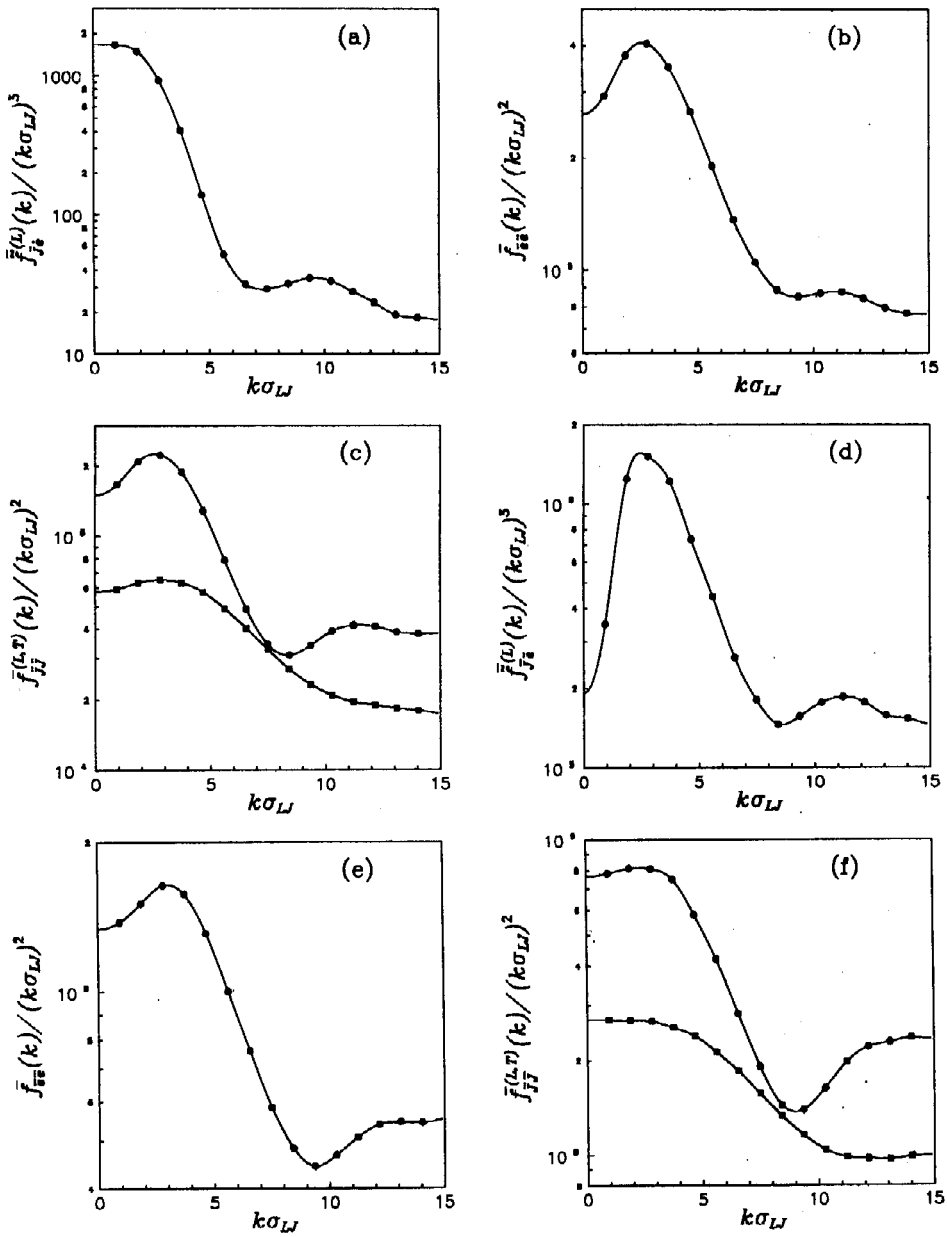

Fig. 2. MD results for the reduced static correlation functions versus wave-vector: **(a)** momentum-energy ($p=2, s=1$); **(b)** energy-energy ($p=s=2$); **(c)** momentum-momentum ($p=s=2$) longitudinal (upper curve) and transverse (lower curve); **(d)** momentum- energy ($p=3, s=2$); **(e)** energy-energy ($p=s=3$); **(f)** momentum-momentum ($p=s=3$) longitudinal (upper curve) and transverse (lower curve).

The MD data for the hydrodynamic correlation times are shown in Fig. 3. These quantities are defined by the following expressions:

$$\tau_{nn}(k) = \frac{1}{f_{nn}(k)} \int_0^\infty f_{nn}(k,t)dt \ , \tag{2.30}$$

$$\tau_{ne}(k) = \frac{1}{f_{ne}(k)} \int_0^\infty f_{ne}(k,t)dt \ , \tag{2.31}$$

$$\tau_{ee}(k) = \frac{1}{f_{ee}(k)} \int_0^\infty f_{ee}(k,t)dt \ , \tag{2.32}$$

$$\tau_{JJ}^{(T)}(k) = \frac{1}{f_{JJ}^{(T)}(k)} \int_0^\infty f_{JJ}^{(T)}(k,t)dt \ . \tag{2.33}$$

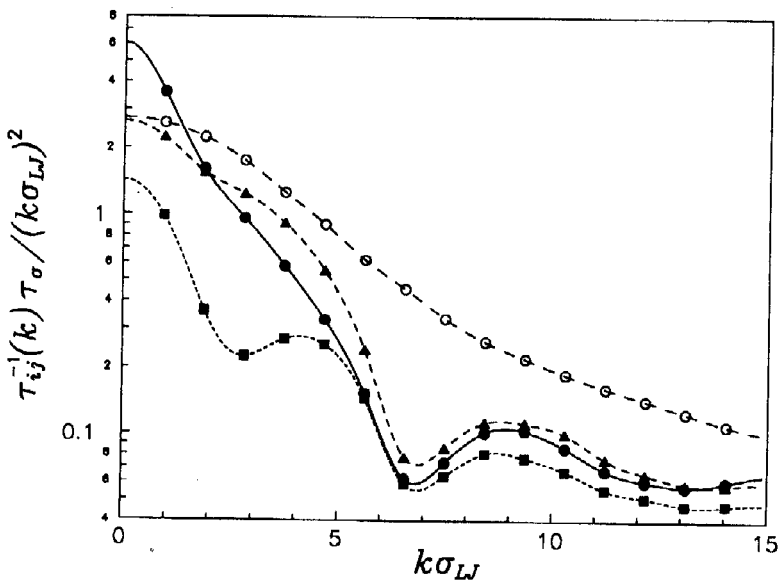

Fig. 3. The reciprocal of the hydrodynamic correlation times as functions of wave-vector: density-density (circles), density-energy (squares), energy-energy (triangles) and transverse momentum-momentum (open circles).

The hydrodynamic correlation times density-density (2,30), density-energy (2.31) and energy-energy (2.32) are connected with longitudinal fluctuations, while momentum-momentum (2.33) corresponds to transverse fluctuations.

The generalized thermodynamic quantities, namely, the generalized enthalpy per particle $h(k)$, the generalized thermal expansion coefficient $\alpha(k)$, the generalized specific heat at constant volume per particle $C_V(k)$ and the ratio of specific heats $\gamma(k)$ at constant pressure and constant volume, are shown in Fig. 4. An analytic representation for these quantities via the SCFs are the following (see, for instance, [2,5])

$$h(k) = \frac{1}{k_B T k}\, \tilde{f}_{je}^{(L)}(k)\,, \tag{2.34}$$

$$C_V(k) = \frac{1}{k_B T^2}\, [f_{ee}(k) - f_{ne}^2(k)/f_{nn}(k)]\,, \tag{2.35}$$

$$\alpha(k)T = \frac{1}{k_B T}\, [h(k) f_{nn}(k) - f_{ne}(k)]\,, \tag{2.36}$$

$$\gamma(k) = \frac{C_P(k)}{C_V(k)}\,, \quad C_P(k) = C_V(k) + k_B T^2 \alpha^2(k)/f_{nn}(k)\,. \tag{2.37}$$

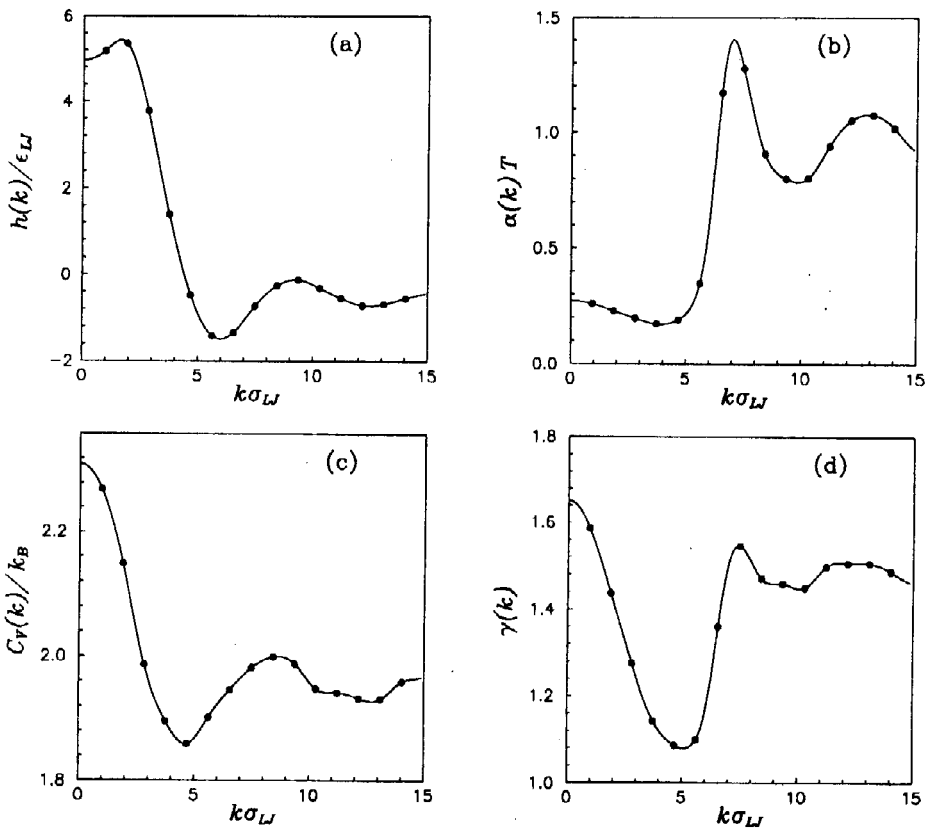

Fig. 4. Generalized thermodynamic quantities as functions of wavevector: **(a)** enthalpy per particle; **(b)** linear-expansion coefficient; **(c)** specific heat at constant volume per particle; **(d)** the ratio of specific heats.

Practically, the results presented in Figs. 1, 2 and 3 give the full information needed for the subsequent calculations of the generalized mode spectrum and the 9×9 longitudinal and 4×4 transverse TCFs, as we shall see later. Moreover, four SCFs and four hydrodynamic correlation times, namely, density-density, density-energy, energy-energy and transverse momentum-momentum, completely determine wave-vector-dependent generalized transport coefficients. In [2] these coefficients and some higher-order SCFs were considered as adjustable parameters for each value of wave-vector using a so-called weighted-squares-fitting procedure to ensure the best fit to MD hydrodynamic TCFs. Obviously, this procedure may lead to unpredictable results that depend on many external factors, such as, for example, choice of set MD TCFS to which the best fit are applied. In our article these quantities are evaluated directly from definitions and free from any external noise.

3. Generalized collective modes and time correlation functions in a markovian approximation

3.1. General theoretic framework

Let us define $F_0(k,t)$ as a $M \times M$ square matrix, each element of which is a TCF. Taking into account the fact that the longitudinal and transverse fluctuations can be studied independently of one another, we should keep in mind that the matrix $F_0(k,t)$ in each specific case is formed by the set of longitudinal or transverse dynamic variables $A(k,t)$ (2.9)-(2.11). These variables satisfy the equation of motion

$$\frac{dA(k,t)}{dt} = iLA(k,t) \tag{3.1a}$$

with a formal solution

$$A(k,t) = e^{iLt}A(k,0) \equiv e^{iLt}A(k)\ , \tag{3.1b}$$

where

$$iL = \sum_{i=1}^{N} \boldsymbol{v}_i \frac{\partial}{\partial \boldsymbol{r}_i} - \frac{1}{m}\sum_{i<j}^{N} \frac{\partial \Phi_{ij}}{\partial \boldsymbol{r}_i}\left(\frac{\partial}{\partial \boldsymbol{v}_i} - \frac{\partial}{\partial \boldsymbol{v}_j}\right) \tag{3.1c}$$

is the Liouville operator.

For longitudinal components the corresponding set is

$$\hat{B}(k) \equiv \hat{B}^{(L)}(k) = col$$

$$\{n(k), J^{(z)}(k), e(k); iLJ^{(z)}(k), iLe(k); (iL)^2J^{(z)}(k), (iL)^2e(k); \ldots\}\ , \tag{3.2a}$$

where $\hat{B}^{(L)}(k)$ is a vector-column with $M = M^{(L)}$ components and $J^{(z)}(k)$ is Z-component of $\boldsymbol{J}(k)$ in the Cartesian system of coordinates. In case of transverse components the vector-column $\hat{B}^{(T)}(k)$ is

$$\hat{B}(k) \equiv \hat{B}^{(T)}(k) = col\{J^{(x,y)}(k), iLJ^{(x,y)}(k), (iL)^2J^{(x,y)}(k), \ldots\} \tag{3.2b}$$

and has $M = M^{(T)}$ components, where $J^{(x,y)}(k)$ is X- or Y-component of $\boldsymbol{J}(k)$. In expressions (3.2) we used that $\boldsymbol{k} = (0,0,k)$.

Then, for the matrix of TCFs

$$F_0(k,t) = \langle \hat{B}(k) e^{-iLt} \hat{B}^+(k) \rangle \tag{3.3}$$

the following equation

$$\frac{\partial}{\partial t} F_0(k,t) - i\Omega(k) F_0(k,t) + \int_0^\infty \phi(k,\tau) F_0(k,t-\tau) d\tau = 0 \tag{3.4}$$

could be derived by different methods. In (3.4) $i\Omega(k)$ and $\phi(k,\tau)$ are the frequency matrix and the matrix of the memory functions, respectively. One way of deriving (3.4) is based on the Mori projection operator method which was used, for instance, in paper [2]. An alternative method is the method of Zubarev's nonequilibrium statistical operator (NSO) [10,11]. By the NSO method, the matrix equation (3.4) has been derived for the set of dynamic variables (3.2a) in [12]. For the matrices $i\Omega(k)$ and $\phi(k,\tau)$ we have

$$i\Omega(k) = \langle iL\hat{B}(k)\hat{B}^+(k) \rangle \langle \hat{B}(k)\hat{B}^+(k) \rangle^{-1} = \frac{\partial}{\partial t} F_0(k,t)|_{t=0} F_0^{-1}(k,0) \,, \tag{3.5}$$

$$\phi(k,\tau) = \langle (1-\mathcal{P}) iL\hat{B}(k) \exp\{-(1-\mathcal{P})iL\tau\} (1-\mathcal{P}) iL\hat{B}^+(k) \rangle \times$$

$$\times \langle \hat{B}(k)\hat{B}^+(k) \rangle^{-1} \,, \tag{3.6}$$

where $\mathcal{P}$ is the Mori projection operator defined as follows

$$\mathcal{P} \ldots = \sum_{k'} \langle \ldots \hat{B}^+(k') \rangle \langle \hat{B}(k')\hat{B}^+(k') \rangle^{-1} \hat{B}(k') \tag{3.7}$$

and

$$F_0(k,0) = \langle \hat{B}(k)\hat{B}^+(k) \rangle \tag{3.8}$$

is the matrix of the SCFs. It should be stressed that according to (3.6) the memory functions have to be calculated with the generalized operator of evolution $\exp\{-(1-\mathcal{P})iL\tau\}$. The alternative representation can be found for $\phi(k,\tau)$ in which the time depending part is described by usual operator of evolution $\exp\{-iL\tau\}$. In this case the derivatives $F_1(k,t) = \frac{\partial}{\partial t} F_0(k,t)$ and $F_2(k,t) = \frac{\partial}{\partial t} F_1(k,t)$ appear. By the NSO method, such representation has been obtained, for example, in Ref.[13]. Then for the Laplace transform of $\phi(k,t)$ we could write

$$\tilde{\phi}(k,z) = \int_0^\infty e^{-zt} \phi(k,t) dt =$$

$$= \{ \tilde{F}_1(k,z) \tilde{F}_0^{-1}(k,z) \tilde{F}_1(k,z) - \tilde{F}_2(k,z) \} F_0^{-1}(k,0) \,, \tag{3.9}$$

where $z = \sigma + i\omega$, $\sigma > 0$ and

$$\tilde{F}_0(k,z) = \int_0^\infty e^{-zt} F_0(k,t)dt \ , \tag{3.10}$$

$$\tilde{F}_1(k,z) = \int_0^\infty e^{-zt} F_1(k,t)dt = z\tilde{F}_0(k,z) - F_0(k,0) \ , \tag{3.11}$$

$$\tilde{F}_2(k,z) = \int_0^\infty e^{-zt} F_2(k,t)dt = z\tilde{F}_1(k,z) - F_1(k,0) \ . \tag{3.12}$$

In terms of the Laplace transform $\tilde{F}_0(k,z)$, the matrix equation (3.4) is

$$[zI - i\Omega(k) + \tilde{\phi}(k,z)]\ \tilde{F}_0(k,z) = F_0(k,0) \ . \tag{3.13}$$

In view of (3.10)-(3.12) and taking into account the explicit expressions (3.5) and (3.9), it can easily be shown that the matrix equation (3.13) is indeed the exact relation.

This is evident from expression (3.6) that, if we choose for $\hat{B}(k)$ the most slowly variables, the elements of the matrix of memory functions constructed on projected variables have to fall faster with time than the elements of matrix $F_0(k,t)$. For example, the hydrodynamic variables (2.9)-(2.11) in the limit $k \to 0$, according to the conservation laws in microcanonical ensemble (2.5)-(2.7), do not depend on time and remain constants, i.e. $\sqrt{N}n(k = 0,t) = N$, $\sqrt{N}\boldsymbol{J}(k = 0,t) = \boldsymbol{J}$ and $\sqrt{N}e(k = 0,t) = E$. This means that Markovian approximation $\tilde{\phi}(k,z) \simeq \tilde{\phi}(k,0)$ for the memory functions can be used as good zero-order approximation. In this case we have

$$\int_0^\infty \phi(k,\tau)F_0(k,t-\tau)d\tau \simeq \int_0^\infty \phi(k,\tau)F_0(k,t)d\tau = \tilde{\phi}(k,z=0)F_0(k,t) \ . \tag{3.14}$$

In a Markovian approximation the equation (3.13) takes the form

$$[zI + T(k)]\ \tilde{F}_M(k,z) = F_0(k,t=0) \ , \tag{3.15}$$

where

$$T(k) = -i\Omega(k) + \tilde{\phi}(k,0) = F_0(k,0)\tilde{F}_0^{-1}(k,0) \tag{3.16}$$

and I is the unit matrix. From the structure of Eqs. (3.13), (3.15) and the form of matrix $T(k)$ it is immediately evident two consequences for $\tilde{F}_M(k,z)$, namely,

$$\tilde{F}_M(k,z=0) = \tilde{F}_0(k,z=0) \ , \tag{3.17}$$

$$\tilde{F}_M(k,z)|_{z\to\infty} = \tilde{F}_0(k,z)|_{z\to\infty} \ . \tag{3.18}$$

The first equality (3.17) states about the coincidence of zero-order moments in t-space for genuine and approximated TCFs, i.e.

$$\int_0^\infty F_M(k,t)dt = \int_0^\infty F_0(k,t)dt \ . \tag{3.19}$$

From (3.18) we have

$$F_M(k,t=0) = F_0(k,t=0) \ , \tag{3.20}$$

i.e. $F_M(k,t)$ in the static limit ($t = 0$) leads directly to exact results. The equalities (3.19) and (3.20) are very important from the view-point of the sum rules. For instance, if the dynamic variable of $(iL)^l\hat{J}^{(z)}(k) \sim (iL)^{l+1}\hat{n}(k)$ is included in the set of (3.2a), one follows from (3.19), (3.20) that the sum rules for TCF of density-density have to be satisfied up to $(2l+2)$-th order. Furthermore, the first moments in time space of the genuine and approximated TCF are equal in magnitude. This statement is valid only in the case when the matrix $\tilde{\phi}(k,0)$ is calculated exactly, or, in other words, the equality (3.19) is satisfied exactly.

Equation (3.15) may be solved analytically in terms of eigenvalues z_α and eigenvectors $\hat{X}_\alpha = \|\hat{X}_{i,\alpha}\|$ of the $T(k)$-matrix

$$\sum_{j=1}^{M} T_{ij}(k)\hat{X}_{j,\alpha} = z_\alpha(k)\hat{X}_{i,\alpha} \ , \tag{3.21}$$

where $i = 1,2,\ldots,M$. Hence we obtain

$$\tilde{F}_M^{ij}(k,z) = \sum_{\alpha=1}^{M} \frac{G_\alpha^{ij}(k)}{z + z_\alpha(k)} \ , \tag{3.22}$$

where

$$G_\alpha^{ij}(k) = \sum_{l=1}^{M} \hat{X}_{i,\alpha}\hat{X}_{\alpha,l}^{-1}F_0^{lj}(k,0) \tag{3.23}$$

and matrix $\hat{X}^{-1}$ is the inverse of $\hat{X} = \|\hat{X}_\alpha\|$. In time-representation the solution (3.22) has the form

$$F_M^{ij}(k,t) = \sum_{\alpha=1}^{M} G_\alpha^{ij}(k)\exp\{-z_\alpha(k)t\} \ , \tag{3.24}$$

i.e. function $F_M^{ij}(k,t)$ can be expressed as a sum of M exponential terms, and each term is connected with effective collective mode $z_\alpha(k)$. The amplitude $G_\alpha^{ij}(k)$ describes a partial contribution of mode $z_\alpha(k)$ in the time correlation function $F_M^{ij}(k,t)$. It is important to note that all quantities in the right-hand side of (3.24) depend only upon k. The expression (3.24) is valid for any M and can be considered as more general formulation of the result obtained previously [2] for $M^{(L)} = 3,5$.

Therefore, in order to find the analytic solutions of (3.24) for TCFs in Markovian approximation, it is necessary to calculate the elements of $T(k)$-matrix. For calculation of $i\Omega(k)$, according to definition (3.5), it is quite sufficient to know the corresponding SCFs, whereas for calculation of the matrix of memory functions $\tilde{\phi}(k,z)$ (or $\phi(k,t)$) some additional information is required. There exist many successful descriptions in the literature (see, for instance, [5–8,14]), which use so-called k- and t-dependent memory functions. The main idea of such method is to find approximate expressions for memory functions using the properties of TCFs, or, alternatively, as approximate solutions of the equations for memory functions and TCFs. Every so often some parameters of approximate memory functions are considered as adjustable parameters to have been found from a fitting procedure for TCFs. In particular, such approach has been applied in paper [2] where the memory functions in Markovian approximation were obtained using a weighted-squares-fitting procedure ensured the best fit to the hydrodynamic TCFs. As mentioned above, the equality (3.19) can be broken in this case, with a consequent violation of higher-order sum rules.

Considering the zero-order moments (3.19) in time space as obtained directly by MD simulations, an alternative method for calculation of the generalized collective mode spectrum and the TCFs can be proposed. In this case, using the properties of the TCFs discussed above, it is easy to show that for description of longitudinal (transverse) fluctuations of a simple fluid it is quite sufficient to calculate the first three (one) zero-order moments $\tilde{F}_0^{ij}(k,0)$ of the TCFs in time space or so-called hydrodynamic correlation times for arbitrary $M^{(L)} \geq 3$ ($M^{(T)} \geq 1$). Following the $T(k)$ matrix can be found from (3.16) and the equation (3.21) for the eigenvalues $z_\alpha(k)$ and eigenvectors $\hat{X}_\alpha$ can be solved. Such approach gives the self-consistent description of the TCFs and ensures the equalities (3.19) and (3.20). Therefore, no adjustable parameters are needed for calculation of $T(k)$. For the investigation of the next approximation in generalized mode description it will be necessary only to find the corresponding higher-order SCFs.

Equations (3.15) and (3.16) together with (3.21)-(3.24) are the key results which will be used in our calculations. However, these equations have yet to be complemented by explicit expressions for matrices $F_0(k) = F_0(k,t=0)$ and $\tilde{F}_0(k,0)$ in order to be applicable to actual calculations. Consider now the cases of longitudinal and transverse fluctuations in more detail.

3.2. Generalized longitudinal collective modes

Choosing the set of initial microscopic variables in the form of (3.2a), we obtain $T(k) = T^{(L)}(k)$, where

$$T^{(L)}(k) = F_0^{(L)}(k,0)[\tilde{F}_0^{(L)}(k,0)]^{-1} \tag{3.25}$$

and

$$F_0^{(L)}(k,t) = \langle \hat{B}^{(L)}(k) e^{-iLt} \hat{B}^{(L)\,+}(k) \rangle \,. \tag{3.26}$$

Taking into account the properties listed in Sec. 2, we can express all elements of matrices $F_0^{(L)}(k) = F_0^{(L)}(k,t=0)$ and $\tilde{F}_0^{(L)}(k,0)$ via the SCFs

and the hydrodynamic correlation times. Then the matrix $F_0^{(L)}(k)$ takes the form

$$\begin{pmatrix}
f_{nn} & 0 & f_{ne} & -ikf_{jJ}^{(L)} & 0 & 0 & -k\tilde{f}_{j\dot{e}}^{(L)} & ikf_{j\ddot{j}}^{(L)} & 0 \\
0 & f_{JJ}^{(L)} & 0 & 0 & -i\tilde{f}_{J\dot{e}}^{(L)} & -f_{J\ddot{j}}^{(L)} & 0 & 0 & i\tilde{f}_{J\ddot{e}}^{(L)} \\
f_{ne} & 0 & f_{ee} & -i\tilde{f}_{je}^{(L)} & 0 & 0 & -f_{\dot{e}\ddot{e}} & i\tilde{f}_{j\ddot{e}}^{(L)} & 0 \\
ikf_{JJ}^{(L)} & 0 & i\tilde{f}_{Je}^{(L)} & f_{j\ddot{j}}^{(L)} & 0 & 0 & -i\tilde{f}_{J\dot{e}}^{(L)} & -f_{j\ddot{j}}^{(L)} & 0 \\
0 & i\tilde{f}_{je}^{(L)} & 0 & 0 & f_{\dot{e}\ddot{e}} & -i\tilde{f}_{j\ddot{e}}^{(L)} & 0 & 0 & -f_{\ddot{e}\ddot{e}} \\
0 & -f_{j\ddot{j}}^{(L)} & 0 & 0 & i\tilde{f}_{J\dot{e}}^{(L)} & f_{J\ddot{j}}^{(L)} & 0 & 0 & -i\tilde{f}_{J\ddot{e}}^{(L)} \\
-k\tilde{f}_{je}^{(L)} & 0 & -f_{\dot{e}\ddot{e}} & i\tilde{f}_{j\dot{e}}^{(L)} & 0 & 0 & f_{\ddot{e}\ddot{e}} & -i\tilde{f}_{\ddot{j}\ddot{e}}^{(L)} & 0 \\
-ikf_{j\ddot{j}}^{(L)} & 0 & -i\tilde{f}_{j\dot{e}}^{(L)} & -f_{J\ddot{j}}^{(L)} & 0 & 0 & i\tilde{f}_{\ddot{j}\ddot{e}}^{(L)} & f_{\ddot{j}\ddot{j}}^{(L)} & 0 \\
0 & -i\tilde{f}_{J\dot{e}}^{(L)} & 0 & 0 & -f_{\ddot{e}\ddot{e}} & i\tilde{f}_{\ddot{j}\ddot{e}}^{(L)} & 0 & 0 & f_{\ddot{e}\ddot{e}}
\end{pmatrix}$$

where $M^{(L)} = 9$ and we put $m = 1$. $F_0^{(L)}(k)$ is a Hermitian matrix.

Similarly, $\tilde{F}_0^{(L)}(k,0)$ has the form

$$\begin{pmatrix}
\tau_{nn}f_{nn} & \frac{i}{k}f_{nn} & \tau_{ne}f_{ne} & 0 & f_{ne} & -ikf_{jJ}^{(L)} & 0 & 0 & -k\tilde{f}_{j\dot{e}}^{(L)} \\
\frac{i}{k}f_{nn} & 0 & \frac{i}{k}f_{ne} & f_{JJ}^{(L)} & 0 & 0 & -i\tilde{f}_{Je}^{(L)} & -f_{J\ddot{j}}^{(L)} & 0 \\
\tau_{ne}f_{ne} & \frac{i}{k}f_{ne} & \tau_{ee}f_{ee} & 0 & f_{ee} & -i\tilde{f}_{je}^{(L)} & 0 & 0 & -f_{\dot{e}\ddot{e}} \\
0 & -f_{JJ}^{(L)} & 0 & 0 & i\tilde{f}_{Je}^{(L)} & f_{J\ddot{j}}^{(L)} & 0 & 0 & -i\tilde{f}_{J\ddot{e}}^{(L)} \\
-f_{ne} & 0 & -f_{ee} & i\tilde{f}_{je}^{(L)} & 0 & 0 & f_{\dot{e}\ddot{e}} & -i\tilde{f}_{j\ddot{e}}^{(L)} & 0 \\
-ikf_{jJ}^{(L)} & 0 & -i\tilde{f}_{je}^{(L)} & -f_{j\ddot{j}}^{(L)} & 0 & 0 & i\tilde{f}_{j\ddot{e}}^{(L)} & f_{j\ddot{j}}^{(L)} & 0 \\
0 & -i\tilde{f}_{Je}^{(L)} & 0 & 0 & -f_{\dot{e}\ddot{e}} & i\tilde{f}_{J\ddot{e}}^{(L)} & 0 & 0 & f_{\ddot{e}\ddot{e}} \\
0 & f_{j\ddot{j}}^{(L)} & 0 & 0 & -i\tilde{f}_{J\dot{e}}^{(L)} & -f_{J\ddot{j}}^{(L)} & 0 & 0 & i\tilde{f}_{J\ddot{e}}^{(L)} \\
k\tilde{f}_{je}^{(L)} & 0 & f_{\dot{e}\ddot{e}} & -i\tilde{f}_{j\dot{e}}^{(L)} & 0 & 0 & -f_{\ddot{e}\ddot{e}} & i\tilde{f}_{\ddot{j}\ddot{e}}^{(L)} & 0
\end{pmatrix}$$

Now we are in a position to perform the calculations using MD data for the SCFs from the base set and for the hydrodynamic correlation times.

The obtained results for the generalized longitudinal collective modes in five-, seven- and nine-mode approximations are presented in Figs. 5, 6. Using the terminology proposed in [1,2], we see that there are two types

of generalized collective modes. Of all the eigenvalues of $T^{(L)}(k)$, three eigenvalues vanish when k goes to zero. They reduce to three hydrodynamic modes independently of $M^{(L)}$ and have the same asymptotic behavior in this limit.

The three generalized hydrodynamic modes are the following:

(**a**) *two propagating sound modes* with the eigenvalues

$$z_s^{(1,2)}(k) = \sigma_s(k) \pm i\omega_s(k) \tag{3.27}$$

for which in the hydrodynamic limit $k \to 0$ we have the well-known result

$$\sigma_s(k) \simeq \Gamma k^2 \ , \quad \omega_s(k) \simeq Ck \ , \tag{3.28}$$

where Γ is the sound-damping coefficient and C is the adiabatic velocity of sound as given by linear hydrodynamics. The results of calculations for the sound propagation $\omega_s(k)$ and the sound damping $\sigma_s(k)$ as functions of wave vector k are shown in Fig. 5a and Fig. 5b, respectively.

(**b**) *a heat mode* with pure real eigenvalue

$$z_h(k) = \sigma_h(k) \tag{3.29}$$

for which in the hydrodynamic limit we have

$$\sigma_h(k) \simeq D_T k^2 \ , \tag{3.30}$$

where D_T is the thermal diffusivity. The obtained results for $\sigma_h(k)$ are shown in Fig. 5c.

We see in Figs. 5a, 5b, and 5c that the results for eigenvalues of the generalized hydrodynamic modes have the tendency to convergence with increasing of $M^{(L)}$.

It is necessary also to note that as pointed out in [2] the results for eigenvalue of generalized heat mode are practically the same for any considered $M^{(L)}$ around $k\sigma_{LJ} \simeq 6$ where the static structure factor $S(k) \equiv f_{nn}(k)$ has the first maximum. The reason is that the coupling of density and energy fluctuations (proportional to $[\gamma(k) - 1]$) is weak at this range, as is seen in Fig. 4d, and hence the viscoelastic theory approach can be used.

All other eigenvalues of $T^{(L)}(k)$ approach finite, real values when k goes to zero (see Figs. 5d, 5f and 6b). They correspond to so-called *kinetic modes* which give the finite damping coefficients for small k and are irrelevant in hydrodynamic limit. Just as in [2], for $M^{(L)} = 5$ we found two kinetic modes $z_K^{(1,2)}(k)$. These modes with dispersion $\omega_K(k)$ and the dampings $\sigma_K^{(1,2)}(k)$ are complex-conjugate for $k\sigma_{LJ} > 1$ ($\sigma_K^{(1)}(k) = \sigma_K^{(2)}(k)$) and pure real for $k\sigma_{LJ} \leq 1$ ($\omega_K(k) = 0$ and $\sigma_K^{(1)}(k) \neq \sigma_K^{(2)}(k)$). In contrary to the previous results [2] where the kinetic modes were observed as real up $k\sigma_{LJ} = 3.5$ as well as in the regions $5.5 < k\sigma_{LJ} < 6.0$ and $10.5 < k\sigma_{LJ} < 11.0$, we found a pure diffusive behavior of kinetic modes only for $k\sigma_{LJ} \leq 1$. For $M^{(L)} = 7$ we obtained additionally two new kinetic modes and behavior of the previously discussed kinetic modes slightly changed. The corresponding results are given in Figs. 5e and 5f. For $M^{(L)} = 9$ we have six kinetic modes. They are presented in Figs. 6a, 6b. We note that the kinetic modes change with $M^{(L)}$ in a seemingly arbitrary and nonconvergent way, much like as observed in hard-sphere fluids [1].

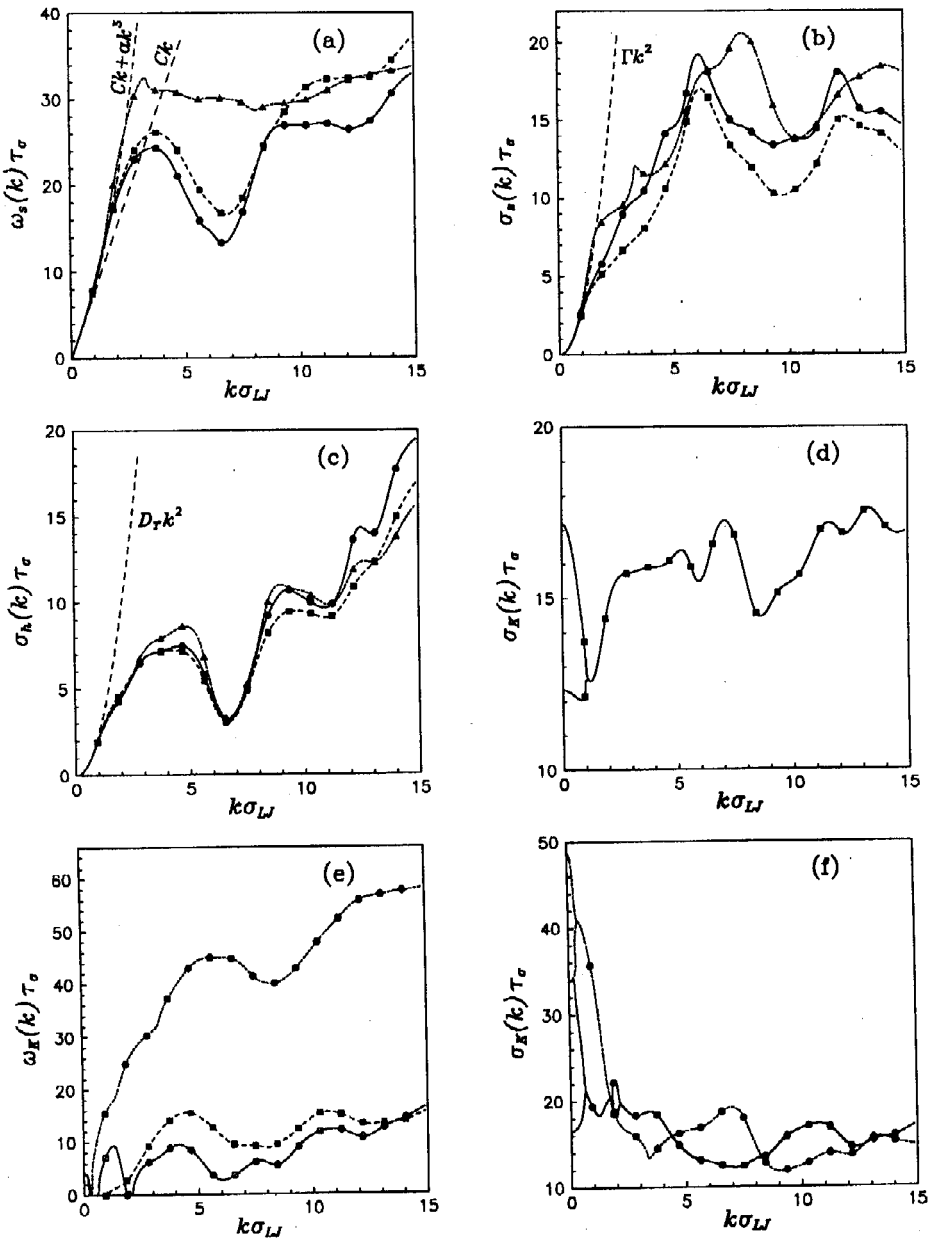

Fig. 5. Generalized longitudinal mode spectrum of a LJ fluid at $n^* = 0.845$ and $T^* = 1.706$: **(a)** sound dispersion; **(b)** sound damping; **(c)** heat mode (results of five-, seven- and nine-mode approximations are shown as squares, triangles and circles, respectively); **(d)** dampings of kinetic modes for five-modes; **(e)** dispersions of kinetic modes for five-(squares) and seven-(circles) modes; **(f)** dampings of kinetic modes for seven-modes.

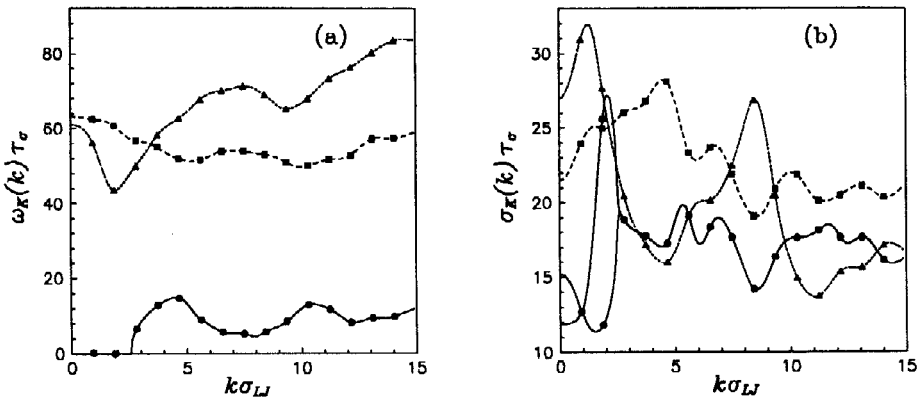

Fig. 6. Generalized longitudinal mode spectrum of a LJ fluid at $n^* = 0.845$ and $T^* = 1.706$: **(a)** dispersions and **(b)** dampings of kinetic modes for nine-mode approximation.

It should be particularly emphasized that the real parts of the hydrodynamic eigenvalues are less than the real parts of all kinetic eigenvalues and remain well separated from them as long as $k\sigma_{LJ} < 3$. Thereafter the generalized sound modes mix with kinetic modes and the last ones mix each other in complicated way. Such result is also closely similar to that in hard-sphere fluids [1].

The results presented in this article for collective mode spectra in the cases $M^{(L)} = 5,7$ and $M^{(T)} = 2,3$ coincide with the corresponding ones of paper [3] in grid points for wave-vector. But for intermediate values between the grid points and extrapolation to $k \to 0$ we used here somewhat advanced procedure which allows to identify modes between themselves with more accuracy. As a result in the case of $M^{(L)} = 7$ some modes for medium and large values of wave-vector are classified here more correctly than in [3].

3.3. Generalized transverse collective modes

For investigation of the generalized transverse modes the initial set of microscopic variables can be taken in form (3.2b). Then we obtain for $T(k) = T^{(T)}(k)$

$$T^{(T)}(k) = F_0^{(T)}(k,0)[\tilde{F}_0^{(T)}(k,0)]^{-1} , \qquad (3.31)$$

where

$$F_0^{(T)}(k,t) = \langle \hat{B}^{(T)}(k) e^{-iLt} \hat{B}^{(T)\,+}(k) \rangle . \qquad (3.32)$$

The matrices $F_0^{(T)}(k) \equiv F_0^{(T)}(k,0)$ and $\tilde{F}_0^{(T)}(k,0)$, using the properties of TCFs, can be written in the following forms

$$F_0^{(T)}(k) = \begin{pmatrix} f_{JJ}^{(T)}(k) & 0 & -f_{J\dot{J}}^{(T)}(k) & 0 \\ 0 & f_{\dot{J}\dot{J}}^{(T)}(k) & 0 & -f_{\dot{J}\ddot{J}}^{(T)}(k) \\ -f_{J\dot{J}}^{(T)}(k) & 0 & f_{\dot{J}\ddot{J}}^{(T)}(k) & 0 \\ 0 & -f_{\dot{J}\ddot{J}}^{(T)}(k) & 0 & f_{\ddot{J}\bar{\ddot{J}}}^{(T)}(k) \end{pmatrix}$$

and

$$\tilde{F}_0^{(T)}(k,0) = \begin{pmatrix} \tau_{JJ}^{(T)}(k) f_{JJ}^{(T)}(k) & f_{JJ}^{(T)}(k) & 0 & -f_{J\dot{J}}^{(T)}(k) \\ -f_{JJ}^{(T)}(k) & 0 & f_{\dot{J}\dot{J}}^{(T)}(k) & 0 \\ 0 & -f_{\dot{J}\dot{J}}^{(T)}(k) & 0 & f_{\dot{J}\ddot{J}}^{(T)}(k) \\ f_{J\dot{J}}^{(T)}(k) & 0 & -f_{\dot{J}\ddot{J}}^{(T)}(k) & 0 \end{pmatrix}$$

where $M^{(T)} = 4$. It is easy to see that $F_0^{(T)}(k)$ is a real symmetric matrix and $\tilde{F}_0^{(T)}(k,0)$ is a real anti-symmetric matrix.

The obtained results for the generalized transverse collective modes in two-, three- and four-mode approximations are shown in Fig. 7.

For $M^{(T)} = 1$ *a pure diffusive mode*

$$\sigma_d(k) = \frac{1}{\tau_{JJ}^{(T)}(k)} \tag{3.33}$$

with the well-known asymptotic Dk^2 at $k \to 0$ [7,8], where D is the kinematic shear viscosity, is found (see Fig. 3).

In two-mode description we have two complex-conjugate modes

$$z_d^{(1,2)}(k) = \sigma_d^{(1,2)}(k) \pm i\omega_d(k), \tag{3.34}$$

for $k\sigma_{LJ} > 1.5$ ($\sigma_d^{(1)}(k) = \sigma_d^{(2)}(k)$) or two diffusive modes with pure real eigenvalues for $k\sigma_{LJ} < 1.5$ ($\sigma_d^{(1)}(k) \neq \sigma_d^{(2)}(k)$, $\omega_d(k) = 0$). In hydrodynamic limit an eigenvalue one of them go to zero with asymptotic of Dk^2 and another one gives finite damping coefficient that is typical for *kinetic modes*.

For $M^{(T)} = 3$ the diffusive mode with pure real eigenvalue appears again and *two complex-conjugate kinetic modes* are found everywhere over the region of k. According to the terminology discussed before the first one is so-called the generalized hydrodynamic mode and has the well-known asymptotic behavior when k goes to zero.

Finally, for $M^{(T)} = 4$ we have one hydrodynamic mode with asymptotic of Dk^2 and three kinetic modes.

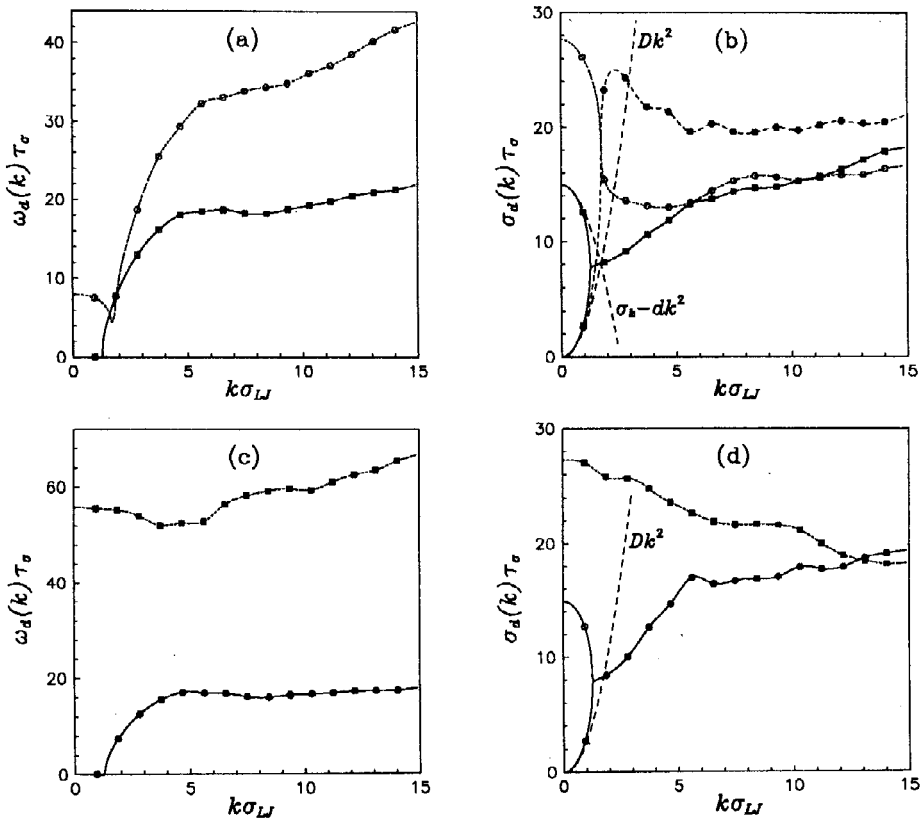

Fig. 7. Generalized transverse mode spectrum of a LJ fluid at $n^* = 0.845$ and $T^* = 1.706$: **(a)** dispersions and **(b)** dampings for two-(squares) and three-(circles) mode approximations; **(c)** dispersions and **(d)** dampings for four-mode approximations.

In view of its importance, we make a few remarks with reference to the behavior of transverse collective modes. First, just as in the case of longitudinal fluctuations, the real part of the hydrodynamic eigenvalue is less than the real parts of the kinetic eigenvalues at range of small k, namely, for $k\sigma_{LJ} < 1$. Thereafter, the mixing with kinetic modes is observed. Second, the question about the existence of propagating transverse modes, discussed previously in literature [8,15], within the conception of generalized modes is solved as follows. The propagating transverse modes for a LJ fluid can be observed as the damping generalized kinetic modes ($M^{(T)} = 3$) for $k\sigma_{LJ} > 1$. For smaller values of k the corresponding collective excitations are overdamped. This is consistent with earlier estimates [8,15] by single-relaxation-time approximation and computer experiments. We see in Fig. 7b that in three-mode description the real part of kinetic eigenvalues is less than the real part of hydrodynamic eigenvalue for $k\sigma_{LJ} > 1.5$, and there

is good indirect evidence that the single-relaxation-time approximation can be used for larger values of k as noted by Levesque *et al* [15]. In two-mode approach the transverse fluctuations are described by two-time relaxation for $k\sigma_{LJ} < 1$ and by the propagating modes for $k\sigma_{LJ} > 1$. In some sense this result is very close to the conclusion of Ref.[15], where it was found that MD data could only be accounted for if one have introduced at finite k's the long-time tail which tends to disappear when k increases.

4. Discussion

In the present paper, the generalized collective mode approach is developed in a form which is free from any adjustable parameters and convenient for the study of higher-order approximations using MD simulations. For the subsequent calculations of the TCFs and collective mode spectrum, one needs only information about the SCFs and the four hydrodynamic correlation times. For comparison with the previous results [2] we have consider nearly the same thermodynamic point, namely, $n^\star = 0.845$ and $T^\star = 1.706$, at our MD simulations. The generalized collective mode spectrum have been calculated for longitudinal fluctuations in the nine-mode description and for transverse fluctuations in the four-mode description. We note that the analysis of the obtained data enable us to make some important conclusions about the dynamical properties of considering system. In particular, as follows from behavior of transverse modes, the shear waves can be observed for $k\sigma_{LJ} > 1$ and these propagating excitations are in fact the kinetic modes.

A weighted least-squares-fitting procedure have been used to determine the memory functions by de Schepper *et al* [2]. This means three transport coefficients were considered as adjustable parameters for each value of k. On the other side, it is necessary to use a fitting procedure for each set of dynamic variables in order to compare five-, seven- and nine-mode approximations. Moreover, a fitting procedure may give results which correlate well with MD data for the lower-order TCFs known from MD experiment, but not so good for the higher-order TCFs. In our approach the memory functions could be determined by the set of the hydrodynamic correlation times and the SCFs. All these quantities have been calculated by MD simulations. The same set of the hydrodynamic correlation times have been used for $M^{(L)} = 5, 7, 9$ and $M^{(T)} = 2, 3, 4$. As far as we known, there are no such data have been published for the cases $M^{(L)} = 9$ and $M^{(T)} = 4$.

It should be particularly emphasized that the proposing approach is closely connected with the memory-function formalism [5,7,8]. The results obtained by this formalism, in particular, for $M^{(L)} = 3$ [5,7,8], $M^{(L)} = 5$ [2,7,12], $M^{(T)} = 1$ and $M^{(T)} = 2$ [7,8], can be reproduced using the set of so-called orthogonal dynamic variables. The orthogonal variables and the variables (3.2) are related to each other by linear transformation. This means that the correct microscopic expressions for the memory functions in a Markovian approximation via the SCFs and the hydrodynamic correlation times can be derived.

The investigation of high-mode spectra gives the possibility to make once more important conclusion. All hydrodynamic and the lowest kinetic

modes converge with increasing of M anywhere in the domain of k-space. In particular, at $k \to 0$ we found the same asymptotic coefficients Γ, C, D_T for $M^{(L)} = 3,5,7,9$ and D for $M^{(T)} = 1,2,3,4$. The results for some thermodynamic and transport quantities in the limit $k \to 0$ are given in Table 2. These quantities were found by extrapolation of the MD data computed at finite values of k to $k = 0$.

Table 2. The thermodynamic and transport properties of a LJ fluid at reduced density $n^* = 0.845$ and reduced temperature $T^* = 1.706$.

Extrapolation	
$S(0) =$	0.049 (0.048)
$h(0)/\epsilon_{LJ} =$	4.96 (5.28)
$\alpha(0)T =$	0.27 (0.25)
$C_V(0)/k_B =$	2.31 (2.33)
$\gamma(0) =$	1.65 (1.55)
$C\tau_\sigma/\sigma_{LJ} =$	7.60 (7.43)
$\Gamma\tau_\sigma/\sigma^2_{LJ} =$	2.98 (2.88)
$D_T\tau_\sigma/\sigma^2_{LJ} =$	2.39 (2.35)
$D\tau_\sigma/\sigma^2_{LJ} =$	2.73
$\lambda\tau_\sigma\sigma_{LJ}/k_B =$	7.69 [8.41]
$\eta\tau_\sigma\sigma_{LJ}/m =$	2.31 [2.28]
$\zeta\tau_\sigma\sigma_{LJ}/m =$	0.64 [0.58]

The results obtained by de Schepper *et al* [2] are given in round brackets. Transport coefficients thermal conductivity λ, shear η and bulk ζ viscosities calculated using Green-Kubo formulas are displayed in square brackets.

Using the results obtained for the generalized collective mode spectrum, we can calculate the 9×9 longitudinal and 4×4 transverse TCFs. As an illustration, we demonstrate here our calculations of the density-density (Fig. 8) and transverse momentum-momentum (Fig. 9) normalized time autocorrelation functions

$$\Phi_{nn}(k,t) = f_{nn}(k,t)/f_{nn}(k)\ , \quad \Phi_{JJ}(k,t)^T = f^{(T)}_{JJ}(k,t)/f^{(T)}_{JJ}(k) \qquad (4.1)$$

for $k = [1,3,5,7,10,15]\,k_{min}$, performed in $M^{(L)} = 5,7,9$ and $M^{(T)} = 2,3,4$

$$f_{nn}(k,t) \simeq \sum_{\alpha=1}^{M^{(L)}} G^{nn}_\alpha(k) e^{-z_\alpha(k)t}\ , \quad f^{(T)}_{JJ}(k,t) \simeq \sum_{\alpha=1}^{M^{(T)}} G^{JJ}_\alpha(k) e^{-z_\alpha(k)t}\ . \qquad (4.2)$$

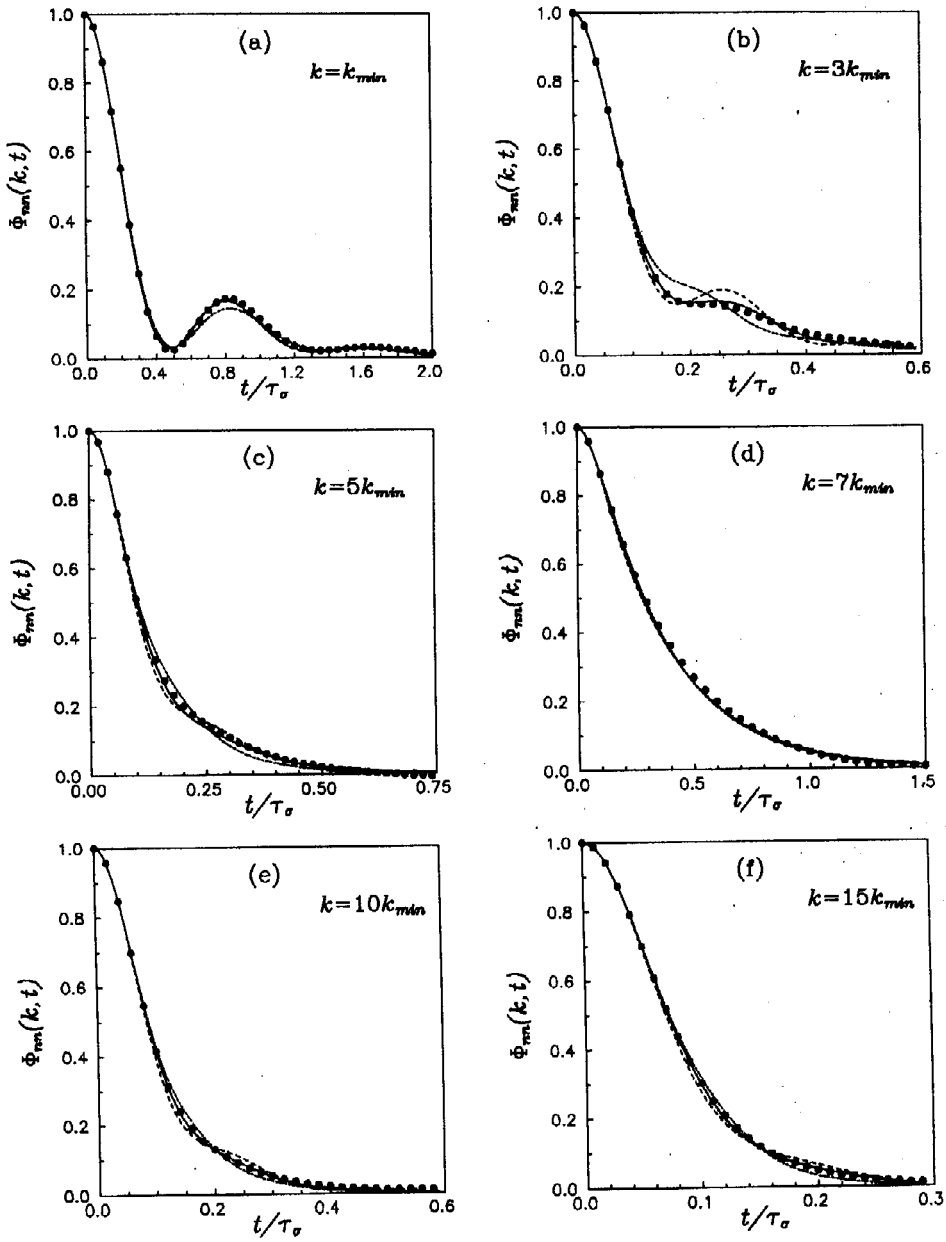

Fig. 8. Density-density normalized time autocorrelation function of a LJ fluid at $n^* = 0.845$ and $T^* = 1.706$ as depending on time t for six fixed values of wave-vector k, namely, $k\sigma_{LJ}$=0.936 **(a)**, 2.807 **(b)**, 4.678 **(c)**, 6.549 **(d)**, 9.355 **(e)**, and 14.033 **(f)**. The results of the five-, seven- and nine-mode approximations are plotted by the long dashed, short dashed and solid curves, respectively. The MD data are shown as circles. For $k\sigma_{LJ}$=6.549 the curves are indistinguishable.

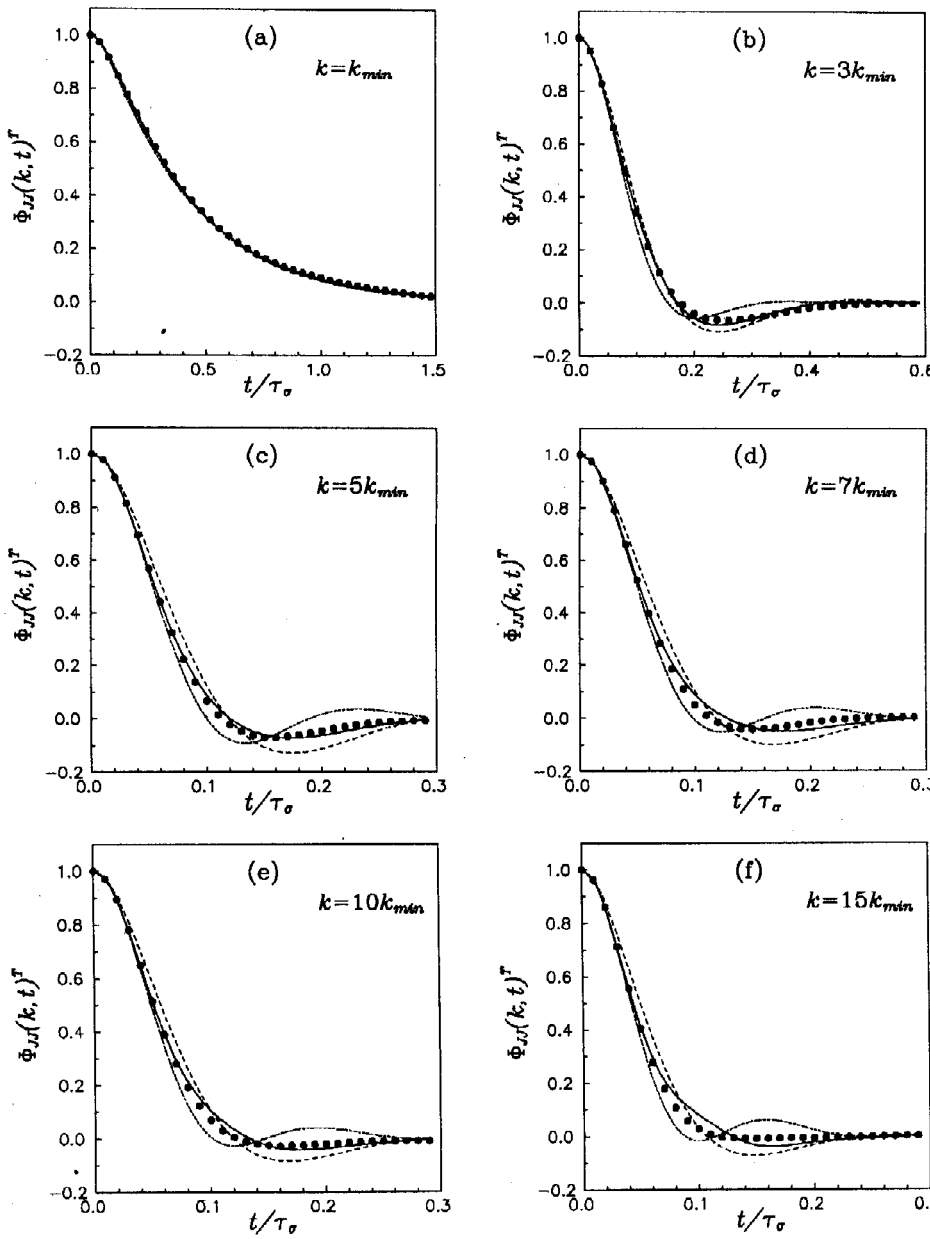

Fig. 9. Momentum-momentum transverse normalized time autocorrelation function of a LJ fluid at $n^* = 0.845$ and $T^* = 1.706$ as depending on time t for six fixed values of wave-vector k, namely, $k\sigma_{LJ}$=0.936 (**a**), 2.807 (**b**), 4.678 (**c**), 6.549 (**d**), 9.355 (**e**), and 14.033 (**f**). The results of the two-, three- and four-mode approximations are plotted by the long dashed, short dashed and solid curves, respectively. The MD data are shown as circles. For $k\sigma_{LJ}$=0.936 the curves are indistinguishable.

The dynamic structure factor

$$S(k,\omega) = \frac{1}{\pi}\mathrm{Re}\int_0^\infty \exp(-i\omega t) f_{nn}(k,t)dt \tag{4.3}$$

performed in five-, seven- and nine-mode approximations

$$S(k,\omega) \simeq \frac{1}{\pi}\mathrm{Re}\sum_{\alpha=1}^{M^{(L)}} \frac{G_\alpha^{nn}(k)}{i\omega + z_\alpha(k)} \tag{4.4}$$

is shown in Fig. 10.

As an example of calculations for the generalized transport coefficients, we consider the wave-vector- and frequency-dependent shear viscosity which is connected with transverse fluctuations

$$\eta(k,\omega) = \frac{nm}{k^2}\tilde{\phi}_{JJ}^{(T)}(k, z = i\omega) \ , \tag{4.5}$$

where the memory function can be expressed in terms of time correlation function as follows

$$\tilde{\phi}_{JJ}^{(T)}(k, z = i\omega) = \left[\int_0^\infty e^{-i\omega t}\Phi_{JJ}(k,t)^T dt\right]^{-1} - i\omega \ . \tag{4.6}$$

Wave-vector-dependent shear viscosity

$$\eta(k) = \eta(k,\omega = 0) = \frac{nm}{k^2}\frac{1}{\tau_{JJ}^{(T)}(k)} \tag{4.7}$$

is directly connected with the transverse momentum-momentum hydrodynamic correlation time (2.33) (Fig. 3). In the generalized mode approach we have obtained

$$\eta(k,\omega) \simeq \frac{nm}{k^2}\left(\sum_{\alpha=1}^{M^{(T)}} G_\alpha^{JJ}(k)\left[\sum_{\alpha=1}^{M^{(T)}} \frac{G_\alpha^{JJ}(k)}{i\omega + z_\alpha(k)}\right]^{-1} - i\omega\right) \tag{4.8}$$

for $M^{(T)} = 2,3,4$. Real $\eta'(k,\omega)$ and imaginary $\eta''(k,\omega)$ parts of the generalized shear viscosity $\eta(k,\omega) = \eta'(k,\omega) - i\eta''(k,\omega)$ are shown in Figs. 11 and 12, respectively.

As we can see in Figs. 8–12, the accuracy of calculations increases as the order of M increases. In the range of the first maximum of the static structure factor ($k \simeq 7k_{min}$), the results for the density-density time correlation function (Fig. 8) and dynamic structure factor (Fig. 10) depend almost not at all on the order $M^{(L)}$ of used approximation. This fact is consistent with the previous results [2] and favours the view that a self-diffusion process dominates the relaxation of density fluctuations for $k\sigma_{LJ} \simeq 2\pi$ where $S(k)$ has a sharp maximum. In the range of $k \simeq k_{min}$ the results for the momentum-momentum transverse time correlation function (Fig. 9) depend

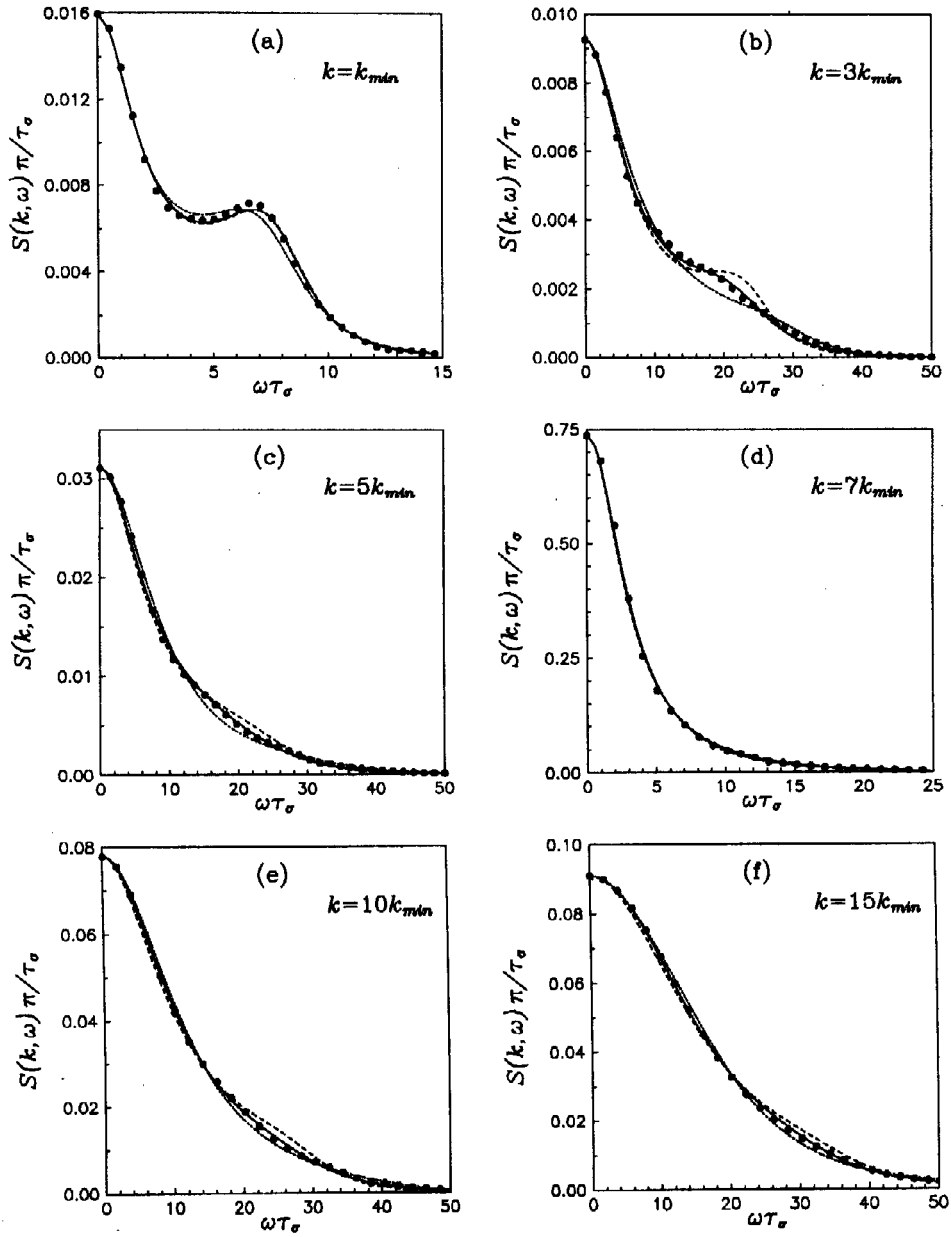

Fig. 10. Dynamic structure factor of a LJ fluid at $n^\star = 0.845$ and $T^\star = 1.706$ as a function of frequency ω for six values of wave-vector k, namely, $k\sigma_{LJ}$=0.936 (**a**), 2.807 (**b**), 4.678 (**c**), 6.549 (**d**), 9.355 (**e**), and 14.033 (**f**). The results of the five-, seven- and nine-mode approximations are plotted by the long dashed, short dashed and solid curves, respectively. The MD data are shown as circles. For $k\sigma_{LJ}$=6.549 the curves are indistinguishable.

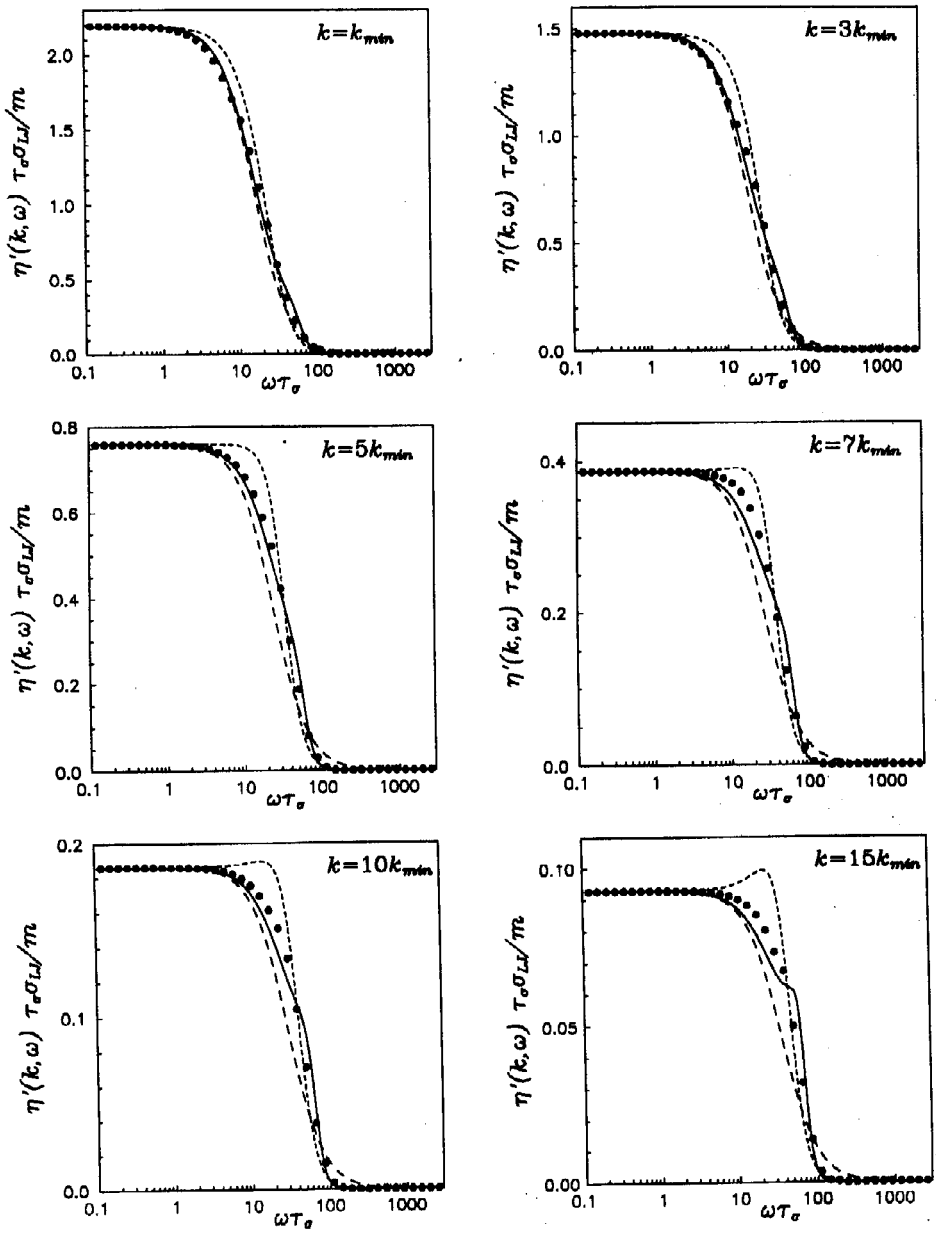

Fig. 11. Shear viscosity (real part) of a LJ fluid at $n^* = 0.845$ and $T^* = 1.706$ as a function of frequency ω for six values of wave-vector k. The results of the two-, three- and four-mode approximations are plotted by the long dashed, short dashed and solid curves, respectively. The MD data are shown as circles.

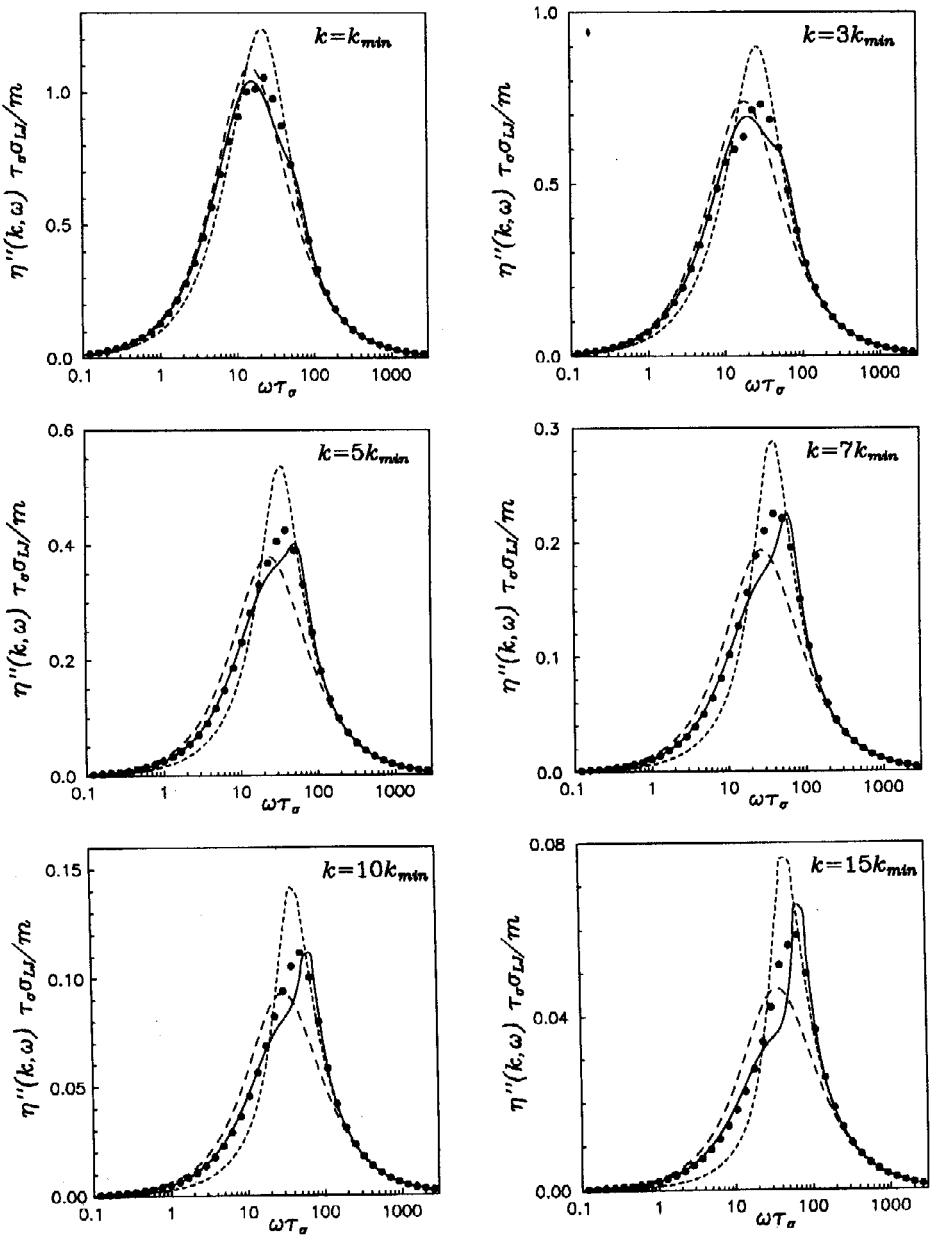

Fig. 12. Shear viscosity (imaginary part) of a LJ fluid at $n^* = 0.845$ and $T^* = 1.706$ as a function of frequency ω for six values of wave-vector k. The results of the two-, three- and four-mode approximations are plotted by the long dashed, short dashed and solid curves, respectively. The MD data are shown as circles.

almost not at all on the order of $M^{(T)}$. However, the generalized shear viscosity (Figs. 11, 12) exhibits more sensitive behavior with respect to the order of used approximation.

A comparison between the results of the generalized mode approach and MD data shows that in the nine-(four-) mode approximation investigated quantities can be described with the higher degree of accuracy everywhere over the region of wave-vector k. Such high-order approximation is already quite sufficient to describe dynamical properties of the system because achieved precision is of order a few per cent just as in the direct MD calculations.

Similar results are obtained for the all other TCFs as well as for the generalized transport coefficients. The report about our studies of these quantities will be given in a separate publication.

Acknowledgments

This work was supported, in part, by Soros Humanitarian Foundations Grant awarded by the American Physical Society. One of us (I.M.) thanks the Austrian Ministry of Science and Research for financial support.

References

[1] Kamgar-Parsi B., Cohen E. G. D., and de Schepper I.M. Dynamic processes in hard-sphere fluids. // Phys. Rev. A, 1987, vol. 35, No 11, p. 4781-4795.

[2] de Schepper I. M., Cohen E. G. D., Bruin C., van Rijs J. C., Montfrooij W., and de Graaf L. A. Hydrodynamic time correlation functions for a Lennard-Jones fluid. // Phys. Rev. A, 1988, vol. 38, No 1, p. 271-287.

[3] Mryglod I. M., Omelyan I. P., Tokarchyk M. V. Generalized collective modes for the Lennard-Jones fluid. // Mol. Phys., 1995, vol. 84, No 2, p. 235-259.

[4] Alley W. E., Alder B. J. Generalized transport coefficients for hard spheres. // Phys. Rev. A, 1983, vol. 27, No 6, p. 3158-3173.

[5] Copley J. R. D., Lovesey S. V. The dynamic properties of monoatomic liquids. // Rep. Prog. Phys., 1975, vol. 38, No 4, p. 461-563.

[6] Lovesey S. V. Density fluctuations in simple fluids. // Z. Phys. B, 1985, vol. 58, p. 79-82.

[7] Boon J. P., Yip S. Molecular Hydrodynamics. N.-Y., McGraw-Hill, 1980.

[8] Hansen J. P., McDonald I. R. Theory of Simple Liquids. Acad. Press, 1987.

[9] van Well A. A., de Graaf L. A. Density fluctuations in liquid argon. II. Coherent dynamic structure factor at large wave numbers. // Phys. Rev. A, 1985, vol. 32, No 4, p. 2384-2395.

[10] Zubarev D. N. Nonequilibrium Statistical Thermodynamics. N.-Y., Consultant Bureau, 1974.

[11] Zubarev D. N. Modern Methods of the Statistical Theory of Nonequilibrium Processes, In: Itogi Nauki i Tekhniki, Sovr. Prob. Mat. (VINITI), 1980, vol. 15, p. 131 (in Russ.).

[12] Mryglod I. M., Tokarchyk M. V. On the statistical hydrodynamics of simple fluids. The generalized transport coefficients. Lviv, 1992. Preprint Inst. for Cond.Matter Phys., ICMP-92-6U, 24 p. (in Ukr.).

[13] Kalashnikov V. P. Linear relaxation equations in the method of nonequilibrium statistical operator. // Teor. Mat. Fiz., 1978, vol. 34, No 3, p. 412-425.

[14] Sjodin S., and Sjolander A. Kinetic model for classical liquids. // Phys. Rev. A, 1978, vol. 18, No 4, p. 1723-1736.

[15] Levesque D., Verlet L., and Kürkijarvi J. Computer "experiment" on classical fluids. IV. Transport properties and time-correlation functions of the Lennard-Jones liquid near its triple point. // Phys. Rev. A, 1973, vol. 7, No 5, p. 1690-1700.

УЗАГАЛЬНЕНІ КОЛЕКТИВНІ МОДИ ЛЕНАРД-ДЖОНСІВСЬКОЇ РІДИНИ. ВИСОКОМОДОВЕ НАБЛИЖЕННЯ

І.П. Омелян, І.М. Мриглод

Запропонований раніше підхід узагальнених колективних мод для дослідження часових кореляційних функцій густих рідин поширено до наближень вищого порядку. Методом молекулярної динаміки пораховано спектр узагальнених колективних мод ленард-джонсівської рідини при дев'ятимодовому описі для повздовжніх флуктуацій та чотиримодовому наближенні для поперечних флуктуацій. Результати отримано як функції хвильового вектора. Для повздовжніх флуктуацій знайдено додатково ще чотири нових кінетичних моди до відомих раніше п'яти. Для поперечних флуктуацій знайдено узагальнену гідродинамічну й три кінетичні моди. Проведено порівняння попередніх робіт з результатами наближень нижчого порядку.